Investigations of Orogenic Gold Deposits in the Cariboo Gold District, East-Central British Columbia (Parts of NTS 093A, H): Progress Report

D.A. Rhys, Panterra Geoservices Inc., Surrey, BC

J.K. Mortensen, University of British Columbia, Vancouver, BC, jmortensen@eos.ubc.ca

K. Ross, Panterra Geoservices Inc., Surrey, BC

Rhys, D.A., Mortensen, J.K. and Ross, K. (2009): Investigations of orogenic gold deposits in the Cariboo gold district, east-central British Columbia (parts of NTS 093A, H): progress report; *in* Geoscience BC Summary of Activities 2008, Geoscience BC, Report 2009-1, p. 49–74.

Introduction

The famous Cariboo Au rush in east-central BC was triggered by the discovery of rich placer-Au deposits on several creeks in the Likely and Wells-Barkerville areas (Figure 1) between 1859 and 1862. This area has subsequently yielded an estimated 2.5 to 3 million ounces (80–96 tonnes) of placer Au (e.g., Levson and Giles, 1993), roughly half of BC's total historic placer-Au production. Gold-bearing orogenic gold-quartz veins and associated pyritic replacement deposits in metamorphic rocks of the Barkerville terrane were discovered soon after placer mining began and have produced approximately 1.2 million ounces (38.3 tonnes) of Au since that time. Lode-Au exploration continues in both the Wells-Barkerville area and structurally higher rock units of the Quesnel terrane farther to the south and west, where the Spanish Mountain and Frasergold deposits occur (Figure 1). Together with the Wells-Barkerville area, the Spanish Mountain and Frasergold deposits, and several other areas of Au prospects along and adjacent to placer-Au–bearing creeks in both the Barkerville and Quesnel terranes define the Cariboo Au district (CGD), which includes much of the central and northwestern parts of the 093A map sheet, as well as the southwestern part of the 093H map sheet (Figure 1).

Although individual deposits of the Quesnel terrane differ in character from those in the Barkerville terrane, much of the Au in each of these terranes is contained within quartz-carbonate veins of broadly 'orogenic' vein type (Goldfarb et al., 2005) that are comparable in style and structural timing. In several deposits in these areas, however, older styles of pyritic and quartz-pyrite mineralization that predate these late orogenic veins are developed in close association with the later veins, suggesting mineralization was a protracted or multiphase process. Despite exciting new discoveries that have been made throughout the Cariboo Au district over the past two decades, very limited recent research has been done directly on the deposits in the area.

This report documents the initial results of a one-year, reconnaissance-level study of lode-Au mineralization and potential of the CGD (Figure 1), which began in 2008. The main goals of the study are to provide constraints on the age(s) and structural controls on mineralization in different parts of the CGD. This is being achieved through a synthesis of previous work in the region combined with focused structural, geochronological and Pb isotopic studies of some of the main lode-Au occurrences in the belt. The objective of this work is to improve the understanding of some key aspects of the geology and Au metallogeny of the CGD, providing guidelines to the future exploration of the district and enabling comparisons to other similar Au districts globally.

Regional Geological Framework

The CGD is underlain by parts of four main terranes (Figure 1). Bedrock in most of the northern and eastern parts of the area comprises middle-greenschist– to lower-amphibolite–grade, polydeformed metamorphic rocks of the Barkerville terrane (the northern extension of the Kootenay terrane) and the structurally overlying Cariboo terrane, which are juxtaposed along the northeast-dipping Pleasant Valley thrust fault (Struik, 1987, 1988). The Barkerville and Cariboo terranes are 'pericratonic' in character, comprising mainly metamorphosed equivalents of continent-derived siliciclastic protoliths with interlayered marble units and granitic orthogneiss, and are thought to have formed in close proximity to the western margin of Laurentia. Structurally overlying both the Barkerville and Cariboo terranes in the northern part of the area are mafic volcanic rocks and associated pelagic sedimentary units of the oceanic Antler allochthon, which forms part of the Slide

Keywords: *Cariboo gold district, Barkerville terrane, orogenic Au, vein, replacement, intrusion, Ar/Ar geochronology, Pb isotopes*

This publication is also available, free of charge, as colour digital files in Adobe Acrobat® PDF format from the Geoscience BC website: http://www.geosciencebc.com/s/DataReleases.asp.

Mountain terrane. The southwestern margin of the Barkerville terrane is structurally overlain along the Eureka thrust by much less deformed and less metamorphosed volcanic and sedimentary strata of the Quesnel terrane, which in this area consists of mainly Middle–Late Triassic volcanic rocks and phyllitic siliciclastic units. The Crooked amphibolite (Figure 1) occurs as a discontinuous, strongly deformed and metamorphosed lens of mafic metavolcanic rocks and minor serpentinite along the Eureka thrust between the Quesnel terrane and the underlying Barkerville terrane. The nature and terrane affiliation of the Crooked amphibolite is uncertain, with some workers interpreting it to be either a basal unit of the Quesnel terrane (e.g., Bloodgood, 1992; Panteleyev et al., 1996), whereas others consider it to be a thrust-bounded slice of the Slide Mountain terrane that is sandwiched between the underlying Barkerville terrane and the base of the Quesnel terrane (e.g., Ash, 2001; Ray et al., 2001; Ferri and Schiarizza, 2006). Other isolated klippe of mafic metavolcanic rocks of uncertain terrane affiliation overlie Barkerville terrane metamorphic rocks on Hardscrabble Mountain and Island Mountain (Struik, 1988; Ferri and Schiarizza, 2006).

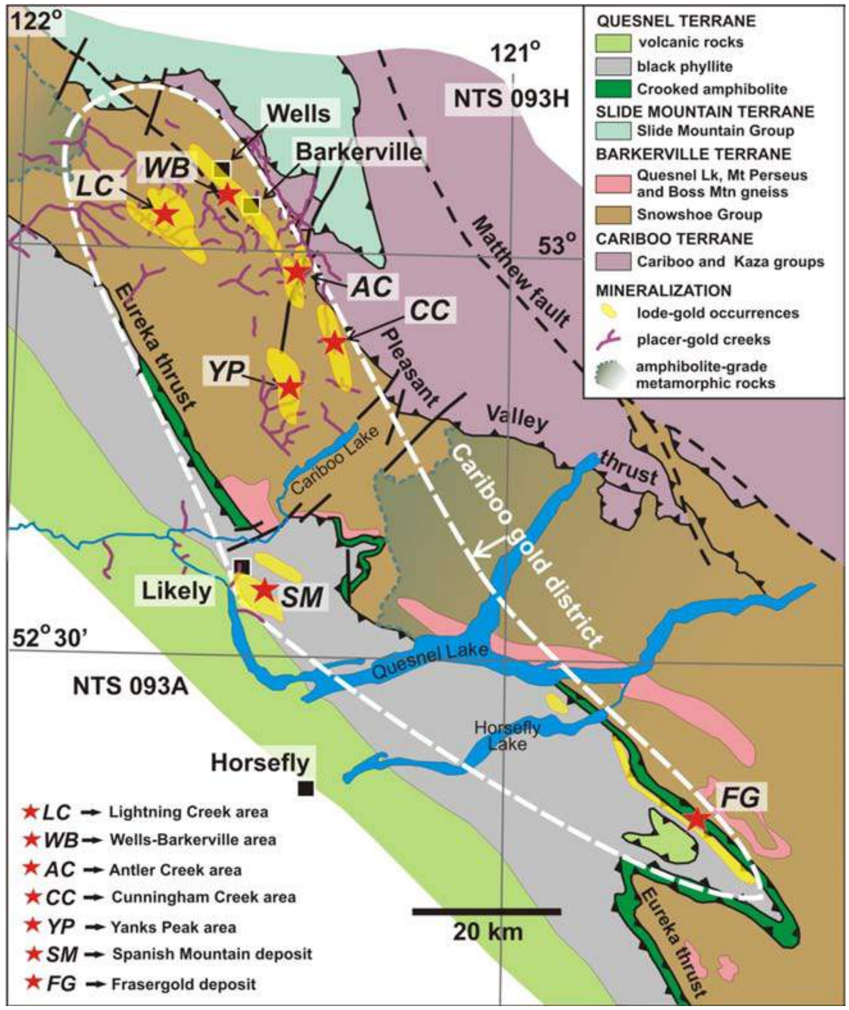

Figure 1: Regional geological setting of the Cariboo Au district, showing principal terranes and major lithological packages. Areas of known lode-Au occurrences are shaded in yellow, and placer-Au–producing creeks are indicated by thick purple lines. Principal known Au-producing areas in the Barkerville terrane are in areas of greenschist-grade metamorphism and do not extend into amphibolite-grade domains.

The Quesnel terrane in this area mainly comprises a package of weakly deformed, variably phyllitic, carbonaceous siliciclastic rocks (locally termed the 'black phyllite' by Rees, 1987; equivalent to the 'black pelite succession' of Logan, 2008) with minor mafic volcanic and volcaniclastic interlayers. This lower, dominantly metaclastic package is overlain along the Spanish thrust (Struik, 1988; Logan, 2008) by mafic to intermediate volcanic rocks assigned to the Late Triassic Nicola Group. The sedimentary package has yielded Middle–Late Triassic fossil ages (Bloodgood, 1992; Panteleyev et al., 1996).

Several suites and ages of intrusive rocks are present in the Wells-Barkerville area and adjoining portions of the Barkerville terrane. Strongly deformed granitic to granodioritic orthogneiss bodies occur in several localities, particularly in the vicinity of Quesnel Lake and east of Eureka Peak (Figure 1). Several of these intrusions have yielded early Mississippian U-Pb zircon crystallization ages (Mortensen et al., 1987; Ferri et al., 1999). Variably foliated metadiorite occurs as small, widespread but volumetrically minor sills, dikes and irregular bodies within the Snowshoe Group of the Barkerville terrane (Struik, 1988; Schiarizza and Ferri, 2003). In rare instances, the metadiorite forms sills up to several hundred metres in thickness. Pickett (2001) and Ray et al. (2001) describe dioritic intrusive rocks in drillcore in the Island Mountain and Mosquito Creek areas, respectively, that may belong to this intrusive suite. Samples of diorite from two localities near Barkerville and one in the Keithley Creek area approximately 30 km to the southeast have given Early Permian U-Pb zircon crystallization ages of 277–281 Ma (Ferri and Friedman, 2002). In the Wells-Barkerville area, several small, strongly altered, foliated felsic bodies termed the Proserpine intrusions have been documented, which appear to have been emplaced prior to the D_2 folding (Struik, 1988; Schiarizza and Ferri, 2003). Younger, rare, locally quartz-phyric rhyolite dikes that appear to be post-tectonic

(Holland, 1954; Struik, 1988) and relatively fresh lamprophyre dikes have also been mapped in several localities in the eastern Barkerville terrane area by Struik (1988) and Termuende (1990). No isotopic age constraints are currently available for the Proserpine intrusions or for the rhyolite or lamprophyre dikes.

Within the black phyllite succession of the Quesnel terrane, several small intrusions that have been mapped southeast of Quesnel Lake range from diorite, monzonite and syenite in composition and are probably Late Triassic to Early Jurassic in age (Panteleyev et al., 1996).

Metamorphic rocks in the CGD record several distinct phases of deformation and metamorphism. Regionally, most workers recognize two dominant syn- to postaccretionary phases of deformation that affect rocks in both the Quesnel and Barkerville terranes, broadly termed phase 1 and phase 2 by previous workers (e.g., Panteleyev et al., 1996; Schiarizza and Ferri, 2003; Ferri and Schiarizza, 2006). Pre-accretionary older fabrics have also been recognized locally in the Barkerville terrane, but are overprinted by the later phase 1 and phase 2 events. Phase 1 structures (generally the earliest recognizable fabrics, termed D_1 here) produced a penetrative slaty to phyllitic cleavage (S_1) that is axial planar to generally east- to northeast-verging, tight to isoclinal, generally northwest-trending F_1 folds and shear zones. The phase 1 (D_1) event is generally thought to be associated with the emplacement of the Nicola Group rocks in the Quesnel terrane onto the Barkerville terrane along the Eureka thrust (Rees, 1987; Bloodgood, 1987, 1992; Panteleyev et al., 1996; Ferri and Schiarizza, 2006). The phase 1 event was accompanied by, and was locally outlasted by peak regional metamorphism. Phase 2 structures (D_2) regionally include the Eureka Peak syncline (Figure 1), which openly refolds both the earlier S_1 foliation and associated folds and the D_1 Eureka thrust (Bloodgood, 1992). The D_2 structures are associated with development of a secondary, locally dominant crenulation cleavage (S_2), which is axial planar to the Eureka syncline and other phase 2 folds (F_2; Bloodgood, 1987, 1992). An intense, shallowly northwest-plunging composite intersection and elongation lineation (L_2) occurs at the intersection of S_2 and older S_1 foliation, and is parallel to F_2 fold axes. The long axes of many Au-bearing zones in the area are parallel to L_2, and extensional veins related to many Au deposits in the area are approximately orthogonal to L_2. Late north- to northeast-trending crenulation cleavage and kink bands form later, retrograde low-strain events regionally.

In the Barkerville terrane, second-phase (F_2) folds form extensive, recumbent and southwest-verging nappe structures that have amplitudes of approximately 25 km (Ferri and Schiarizza, 2006). These result in the overturning of large portions of the Barkerville terrane stratigraphy. They, in turn, are affected by the Lightning Creek anticline and an open, northwest-trending upright fold that runs through central portions of the Barkerville terrane, and to which late (S_3) crenulation cleavage is axial planar.

Structurally late northerly to north-northeasterly trending, right-lateral (dextral) faults occur throughout the CGD, extending across and offsetting lithological contacts including major thrust surfaces associated with terrane boundaries. These faults have a protracted structural history, locally displaying early semibrittle fabrics, with widespread later brittle displacements along clay gouge seams. These structures are often spatially associated with late gold-quartz veins that are widespread throughout the district.

Absolute age constraints on the timing of the various metamorphic and structural events that have affected the Barkerville and Quesnel terranes prior to this study were very limited. Peak metamorphism is thought to have occurred at approximately 174 ±4 Ma, based on a U-Pb age for metamorphic titanite from near Quesnel Lake (Mortensen et al., 1987). Andrew et al. (1983) reported a similar K-Ar whole-rock age of 179 ±8 Ma for phyllite at the Cariboo Gold Quartz mine. Potassium-argon ages of 141 ±5 Ma (Andrew et al., 1983) and 139 ±5 Ma (Alldrick, 1983) have been reported for sericite associated with mineralized quartz veins at the Cariboo Gold Quartz and Mosquito Creek mines, respectively. An essential aspect of understanding the relative timing and controls on Au mineralization throughout the CGD district is whether the different-phased fabrics associated with the principal deformation events and metamorphism summarized above are correlative throughout the region, especially across terrane boundaries. Since the principal fabrics across the region are syn- to postaccretionary in timing, and foliations and associated folds can be traced continuously across the region with similar relative ages, styles and orientations, the sequence of regional deformation is considered here to be correlative between the Quesnel and Barkerville terranes, although absolute ages of each event could vary locally both between and within individual terranes if deformation was transgressive across the area. Ongoing geochronology associated with this study should help to provide further constraints.

Field and Analytical Studies from 2008

Our fieldwork in the CGD included detailed field examination of lode-Au occurrences and collection of an extensive suite of samples for petrographic, dating and geochemical studies. Systematic surface mapping of the Spanish Mountain deposit area in conjunction with drillcore review was also undertaken during the fieldwork program to further understand the setting and controls on mineralization there. A substantial amount of $^{40}Ar/^{39}Ar$ dating has now been completed from the Wells-Barkerville area as part of this study, and four U-Pb zircon ages have also been determined for samples from the Spanish Mountain area. In addition, a number of sulphide samples from the Wells-Barkerville area have been analyzed for Pb isotopic compositions. Results of field studies in the principal field areas that were examined are summarized below in the context of previously published and unpublished work, together with a preliminary interpretation of the results of the new dating and isotopic studies. Additional geochronological, isotopic and petrographic work is currently underway and will be synthesized in future publications.

Lode-Au Deposits in the Barkerville Terrane

The Barkerville terrane hosts the highest frequency of lode-Au occurrences in, and records most of the historical lode Au and placer production from, the CGD. Known lode-Au occurrences are most abundant over an approximately 50 km strike length from Cariboo Lake in the northwest to several kilometres northwest of Wells (Figure 1). Within this area, mineralization occurs in two parallel north-northwest–oriented trends:

> The first trend is located along the northeastern margin of the Barkerville terrane, extending from the Wells-Barkerville area southeastwards through prospects on Antler and then Cunningham creeks (Figure 1).
>
> The second trend lies approximately 10 km to the west-southwest of the above trend in central portions of the Barkerville terrane, and comprises two clusters of lode-Au deposits: the Lightning Creek area in the north and Yanks Peak area to the southeast (Figure 1). Although few Au occurrences are reported between these two areas, numerous quartz veins and vein systems are visible on ridgetops between them.

Principal placer-producing creeks are spatially associated with, or drain the ridges in these trends (Figure 1), suggesting that much of the placer Au is locally sourced. The termination of these mineralized trends before the intersection of the biotite isograd to the southeast of Cariboo Lake and to the west-northwest of Wells (Figure 1) suggests that the associated vein systems may be preferentially localized in lower-greenschist–grade rocks (Struik, 1988). These trends may correspond to structural corridors formed by high-strain zones or faults in the region, within which additional local lithological and structural controls may have focused mineralization.

Wells-Barkerville Area, Barkerville Terrane

The Wells-Barkerville area is by far the most important Au-producing camp within the CGD, having been the source of virtually all historical lode-Au production and much of the placer production from the district (Hall, 1999). Lode-Au production in the camp has come from the Cariboo Gold Quartz (093H 019), Island Mountain (093H 019) and Mosquito Creek (093H 025) mines, which collectively define a single, shallow northwest-plunging mineralizing system that is developed over a 4.5 km strike length, from which 1.23 million ounces of Au have been produced (Hall, 1999). Gold mineralization exhibits both strong structural and stratigraphic control, and is developed mainly within 150 m of the northeast-dipping contact between interbedded quartzite, sericite, phyllite and limestone of the Downey succession to the northeast ('Baker' unit in mine terminology), and carbonaceous metaturbiditic rocks of the Hardscrabble succession to the southwest ('Rainbow' unit). Showings and deposits continue for another 10 km to the southeast from the Cariboo Gold Quartz mine in the same stratigraphic position (e.g., Warspite, Hard Cash, Antler Mountain; Figure 1; Sutherland Brown, 1957). Mineralization is of two varieties, replacement and vein mineralization, which occur together within a broad zone of diffuse iron-carbonate–sericite alteration and high D_2 strain (Skerl, 1948; Sutherland Brown, 1957; Hall, 1999; Rhys and Ross, 2001).

Replacement Mineralization

Replacement mineralization comprises multiple small (500–40 000 tonnes), manto-like, folded, northwest-plunging, rod-shaped bodies of massive, fine-grained pyrite>iron-carbonate+quartz that replace limestone bands within 25 m of the structural base of the Downey (Baker unit) succession in the Island Mountain and Mosquito Creek mines in northwestern portions of the camp (Benedict, 1945; Alldrick, 1983; Robert and Taylor, 1989). Approximately 32% of lode production from the camp was from this mineralization type (Hall, 1999). Ore shoots plunge parallel to the axes of, and are spatially associated with the hinge zones of mesoscopic D_2 folds, at least locally where they are intersected by northeast-dipping S_2-parallel thrust surfaces in zones of higher strain. The pyrite bodies contain coarse-grained dolomite, pyrite and arsenopyrite on their margins (Figure 2a), and are often enveloped by sericite±iron-carbonate/dolomite±fuchsite alteration or silicification, both of which replace the host limestone outward from the pyrite mineralization. Mineralization is commonly banded, with alternating pyrite and carbonate-dominant bands (Figure 2b). Highest Au grades are associated with fine-grained pyrite within which Au occurs as grains along crystal boundaries and fractures.

Replacement mineralization of similar character at the Bonanza Ledge zone (093H 140) occurs 2.25 km to the southeast of the Cariboo Gold Quartz–Mosquito system (Rhys and Ross, 2001; Yin and Daignault, 2007). However, the Bonanza Ledge zone is hosted by, and replaces thinly bedded metaturbidites of the Hardscrabble succession that are approximately 500 m structurally lower than the Rainbow-Baker contact area, which hosts replacement mineralization in the Mosquito and Island Mountain mines. This suggests the potential for stratabound mineralization in other parts of the local stratigraphy. Mineralization in the Bonanza Ledge zone occurs in discrete areas of massive, banded and veinlet pyrite within a 20–100 m wide zone of intense sericite–iron-magnesium-carbonate–pyrite alteration. High-grade mineralization (5–80 g/t Au) occurs in areas locally more than 30 m thick comprising 10–70% pyrite (Figure 2c) in a gangue of muscovite, dolomite-ankerite and quartz, forming at least two crudely shallowly-plunging zones. Gold occurs as 2.5–60 m native grains on fractures or grain boundaries in pyrite with galena and chalcopyrite, or encapsulated in pyrite. Sheeted pale grey veins and silicification occur peripheral to the alteration zone. Gold-bearing zones grade laterally and vertically into sets of non-gold–bearing pyrite–pyrrhotite–chlorite–iron-carbonate veinlets in mauve sericite±albite±chlorite alteration (Figure 2d).

Quartz Vein Mineralization

At least two stages of quartz veining occur in the district, comprising an early, poorly mineralized and deformed set of veins that are cut by later Au-bearing, late-tectonic quartz-carbonate-pyrite veins. The early veins are moderately northeast-dipping, variably deformed quartz±gold-carbonate±muscovite veins that are commonly developed in all three of the principal Wells area mines (Rhys and Ross, 2001). They are characterized by silvery to white muscovite as aggregates and networks in the quartz, as well as blebby, coarse iron-carbonate aggregates, and often have green to silver muscovite alteration envelopes. They are generally low in pyrite content, but pyrite clots occur in some larger veins. The veins range up to 1 m thick, are boudinaged and folded, laterally discontinuous along strike and affected by most or all D_2 strain (Figure 3). These veins contain only background or low (<2 g/t) Au concentrations. In some locations, veins of this type form several generations, which display a gradation in strain state and mineralogy. Although lacking significant Au and predating main-stage quartz veining, they are localized along the same corridor as the later Au-bearing veins and also extend into basal portions of the Baker unit to the northeast. These dif-

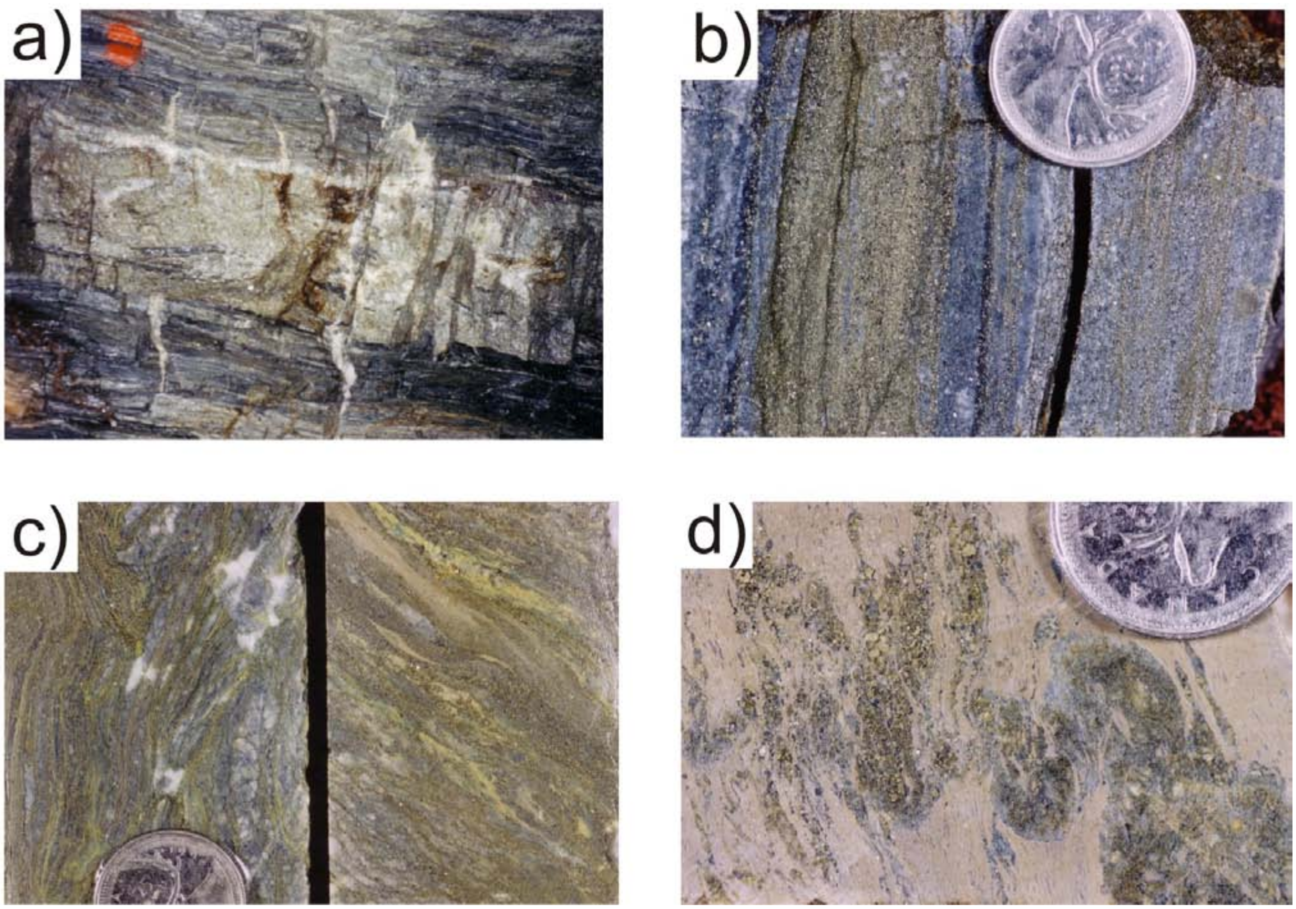

Figure 2: Style of replacement mineralization in the Wells-Barkerville area: **a)** band of pyrite replacement mineralization in the foliated limestone of the Baker unit, 4400 level, Mosquito Creek mine; field of view 2 m; note pale peripheral quartz-carbonate margins to the pyrite and the steeply dipping, northeast-trending quartz extensional veinlets that emanate off the replacement zone; **b)** detail of fine-grained, banded pyritic replacement mineralization in blue-grey dolomitized limestone from the Mosquito mine, 4400 level; **c)** typical replacement-style pyritic mineralization from the Bonanza Ledge zone, showing fine-grained pervasively disseminated pyrite lamina and bands that alternate with dolomitic (left) and tan sericite altered (right) matrix; the protolith was calcareous siltstone (left) and mudstone (right); **d)** Purple-grey peripheral sericite alteration to the Bonanza Ledge zone containing ptygmatically folded pyrite-pyrrhotite veinlets.

fer from the younger, northwest-trending Au-bearing 'strike' veins such as the BC vein, although previous workers have often included them in that set. Relative timing relationships between these older deformed quartz veins and replacement mineralization was not established in the field.

In contrast, main-stage quartz veins associated with Au mineralization are structurally late and postdate all D_1 and much or all D_2 strain in the region. They have been the source of approximately 68% of the lode-Au production in the Wells-Barkerville area (Hall, 1999), comprising almost all of the Au production from the Cariboo Gold Quartz mine and a significant amount from the other two mines. Although individual veins are discordant to stratigraphy, the vein systems as a whole are stratabound and generally confined to 150–250 m of stratigraphy within grey pelitic to psammitic phyllite of the Rainbow unit over the entire >4 km length of the system. The favourable portions of the Rainbow unit lie immediately adjacent to, and to the southwest of the Rainbow-Baker contact area where replacement mineralization is developed, and veins frequently extend up to or into the same horizons as the replacement mineralization (Skerl, 1948).

The Au-bearing veins comprise east-trending, steeply dipping, low displacement sinistral shear veins ('diagonal' veins; Figures 4a, b, 5b) with strike lengths of 20–150 m and coeval, sheeted sets of northeast-trending extensional veins ('orthogonal' or 'transverse' veins; Figures 4c, 5a) that together form complex vein arrays (Skerl, 1948; Sutherland Brown, 1957). Veins consist of white quartz+pyrite with iron-carbonate±muscovite selvages and pyritic cores that often display a two-stage paragenesis from early fibrous carbonate-quartz to younger massive quartz-pyrite in vein cores (Figure 4d). Scheelite and fuchsite are local accessory minerals, and native gold occurs in association with pyrite and locally cosalite and bismuthinite (Skerl, 1948). Extensional transverse veins commonly contain quartz-carbonate fibres aligned perpendicular to vein walls, consistent with dominantly or nearly pure extensional opening (Figure 4d). Adjacent to replacement mineralization, the veins typically cut across it, although in some locations extensional veins may emanate off the margins of pyrite replacement zones (Figure 2a).

Figure 3: Folded early quartz-carbonate vein with muscovite envelopes, Mosquito mine, 4400 level. The vein is within the lower portions of the Baker limestone. Field of view is 1.2 m, and view is southwest of drift wall.

The diagonal veins are commonly distributed en échelon along the favourable Rainbow stratigraphic horizons, and may be linked by, or terminate in horsetail-like arrays of extensional veins. The structural style of veins is dominantly brittle, but local stylolitic pressure-solution seams, sinistral shear bands and sigmoidal shapes to extensional veins support local semibrittle behaviour during vein formation (Figure 4a, b). The most concentrated zones of veining are developed mainly in the Rainbow 1 unit (grey, fine-grained metaturbidite) where north-trending, east-dipping, late-D_2 dextral faults cross the stratigraphy, defining individual mineralized zones of multiple veins that are named after the corresponding faults. Although the veins postdate most D_2 strain and cut across F_2 fold closures, they are kinematically consistent with formation in response to northeast-directed D_2 shortening, and extensional (diagonal) veins in this set are generally oriented orthogonal to the L_2 lineation (Figure 4c), suggesting that they formed in response to extensional opening parallel to L_2, collectively suggesting a late-D_2 timing. Associated north-trending dextral faults may also contain veining and Au mineralization (Richards, 1948), although the faults have typically seen much later brittle displacement that disrupts the veining and has formed significant clay gouge.

A third type of Au-bearing quartz vein is the 'strike' or 'A' vein type, which are more continuous, fault-hosted, northwest-trending and steeply northeast-dipping shear veins (Johnston and Uglow, 1926; Sutherland Brown, 1957). Although not common in the main mine trend, the best examples of this style of veining occur to the southeast of the Cariboo Gold Quartz mine near the Bonanza Ledge zone. The largest vein of this type is the BC vein, which has been traced in outcrop and drilling for 800 m, is locally >30 m thick (Figure 6) and is localized in a carbonaceous phyllite termed the BC unit, which lies approximately 500 m southwest of the Rainbow-Baker contact. Several shallowly northwest-plunging pyritic ore shoots were historically mined from the vein from underground workings connected to the Cariboo Gold Quartz mine. Timing relationships are similar to other Au-bearing veins in the district, with a late timing indicated by its planar nature, and the presence of brecciated wallrock fragments within it that contain rotated S_1 and S_2 foliations, indicating that vein formation continued to late during or after D_2, since D_2 fabrics are affected. The BC vein, like other Au-bearing veins in the district, is spatially associated with older, folded replacement mineralization. The Bonanza Ledge zone occurs between, immediately within, and for up to 50 m into its footwall.

Relationships between Mineralization Types and their Potential Controls

A block model illustrating vein relationships and kinematics of principal Au-bearing veins in the Wells-Barkerville area is illustrated in Figure 5b. Diagonal, sinistral shear veins may be conjugate to the north-trending faults. Transverse extensional veins are developed at a high angle to the northwest-plunging L_2 elongation lineation and probably formed due to extension parallel to L_2. Together, the kinematics, orientations and strain states of the veins and faults suggest that all of these structures formed during inclined northeast-directed shortening, potentially late during D_2. The common occurrence of older deformed quartz veins along the same structural northwest-trending corridors as the Au-bearing veins suggest that the Au-bearing veins represent the culmination of a sequence of quartz veining that may have occurred sporadically during regional D_2 deformation, but until the latter stages was not significantly Au bearing.

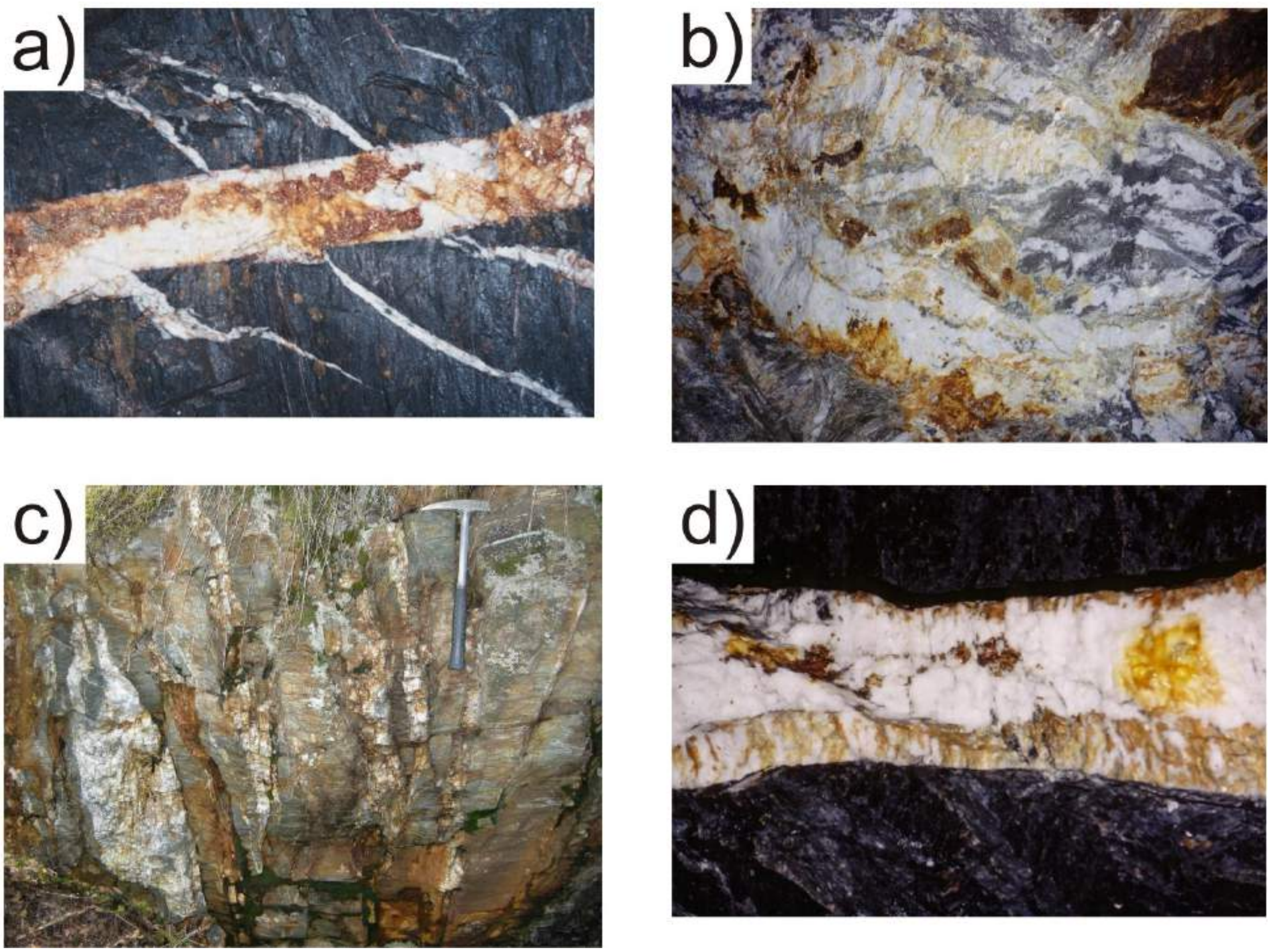

Figure 4: Main-stage Au-bearing quartz vein systems in the Wells-Barkerville area: **a)** east-northeast-trending quartz vein in intermediate orientation between diagonal and transverse vein orientation contains clots of coarse, partially oxidized pyrite, and is obliquely joined by north-northeast-trending extensional veins; angular relationships between the two vein types suggest that the extensional veinlets formed in response to a minor component of sinistral displacement on the principal vein; note that since this is a view up at the back, the apparent shear sense is reversed; field of view = 2 m, Cariboo Gold Quartz mine 1200 level; **b)** mineralized quartz-pyrite fault-fill, east-trending diagonal vein, Mosquito Creek mine, 4400 level; the vein is approximately 0.8 m thick; discrete slip surfaces with pyritic pressure-solution seams disrupt vein surfaces internally and synthetic shear bands oblique to the shear vein walls record an apparent sinistral shear sense; note that the view is up at the back so apparent shear-sense indicators are reversed; the grey banding in the vein is pyrite; **c)** sheeted northeast-trending quartz>pyrite+iron-carbonate extensional veins on the southeast side of Williams Creek at the Blackjack prospect near Barkerville; view is to the northeast; note the shallowly northwest-plunging L_2 lineation on the foliation surfaces (dips shallowly to left) to which the veins are nearly orthogonal; rusty carbonate-pyrite alteration affects the phyllitic wallrocks; hammer for scale; **d)** northeast-trending extensional ('transverse') vein in the Cariboo Gold Quartz mine; two stages of vein filling are apparent: fibrous quartz-carbonate intergrowths aligned at high angles to vein walls form the first, non–Au-bearing veining phase on vein margins, while the central vein fill comprises massive quartz with pyrite clots; view up at the back, Cariboo Gold Quartz mine, 1200 level, Rainbow zone; the vein is 0.3 m thick.

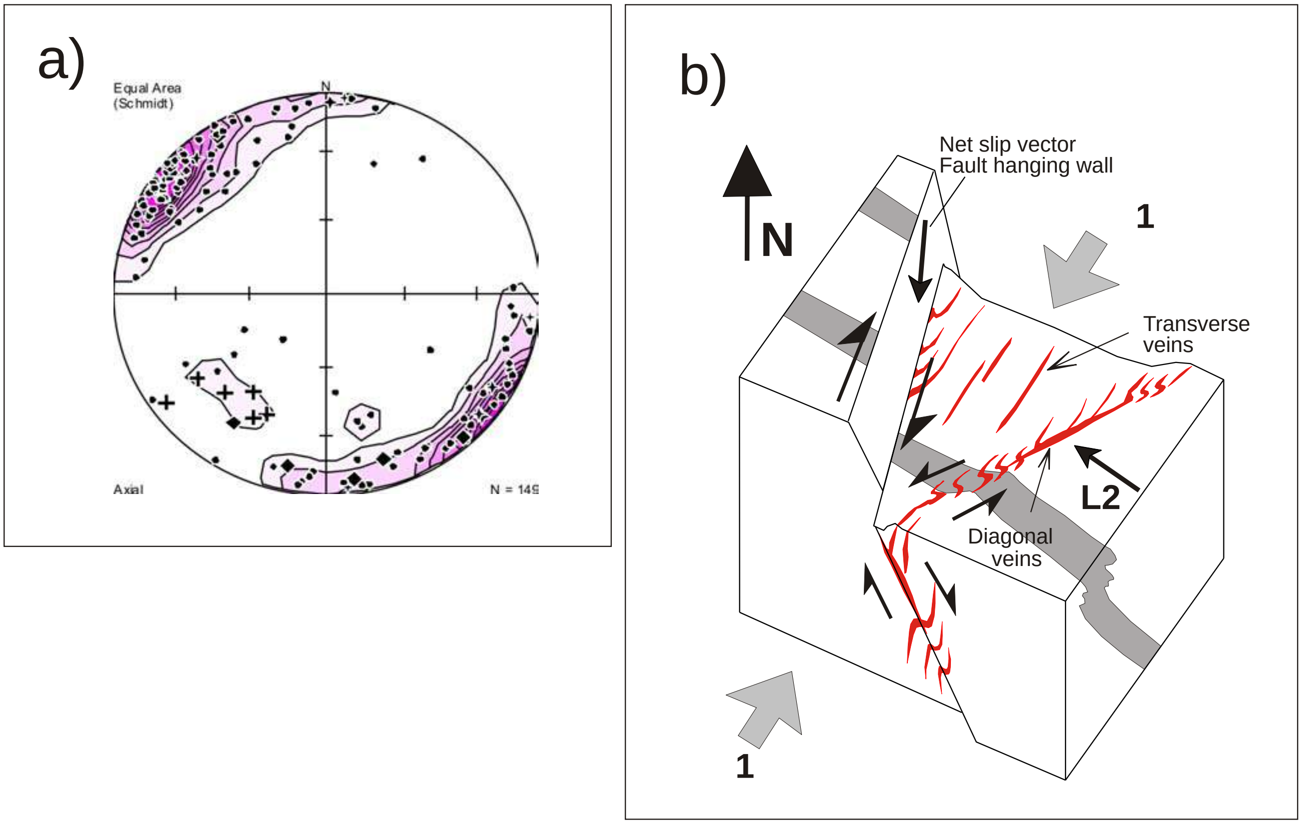

Figure 5: Geometries of Au-bearing veins in the Wells-Barkerville area: **a)** equal-area projection of poles to quartz veins in the central Wells-Barkerville area Au system; data are from underground workings and surface exposures in the Cariboo Gold Quartz and Mosquito mines, and at the surface along Lowhee Creek; symbols are as follows: small dots, extensional veins; diamonds, diagonal veins; large crosses, BC vein; note the dominant steep northeast trends to extensional veins; data are from Rhys and Ross (2001) with additional data collected in 2008; **b)** block model illustrating interpreted relationships between the principal Au-bearing vein sets and north-trending dextral >east-side-down faults in response to inclined northeast-directed shortening.

Figure 6: Surface exposure of the BC vein, a major 'strike' vein, looking southeast. This thick, northwest-trending fault-fill vein hosts several ore shoots and lies directly adjacent to the Bonanza Ledge zone. Note person for scale (right).

There has been much speculation regarding the relationships between the replacement and vein styles of mineralization in the Wells-Barkerville area (e.g., Benedict, 1945; Robert and Taylor, 1989). The replacement mineralization is clearly strained, but in the absence of definite strain markers it is uncertain whether it is affected by both D_1 and D_2 strains, or only by the latter event. The occurrence of the replacement mineralization in F_2 fold hinges and the overall plunge of the mineralization parallel to those folds may imply syn-D_2 timing, although the tectonic focus of earlier mineralization into the fold hinges is also possible.

The close spatial association of the replacement and later vein mineralization in a single, northwest-plunging mineralizing system could imply 1) a genetic link, representing different products of a single, long-lived, synmetamorphic and syn-Jurassic deformational and mineralizing event; 2) a two-stage mineralizing process whereby vein-hosted mineralization was remobilized from older Au-enriched replacement ores late in the structural history or 3) the replacement and Au-bearing veining episodes represent independent and temporally separate mineralizing events that both introduced Au into respective areas but were controlled by common structural and fluid channels that were subject to later remobilization. Pure *in situ* or short-distance remobilization of Au into the later veins from replacement mineralization is unlikely, since the quartz veins are significantly greater producers, and are far more geographically extensive, both within the Wells-Barkerville area and in other lode-Au–bearing areas throughout the Barkerville terrane. In addition, remobilization does not explain the preferential development of the quartz veins themselves, which rapidly diminish in abundance outside the northwest-plunging zones of replacement mineralization. The spatial association instead implies a common control on fluid flow in the mineralizing system. Further work will attempt to evaluate the relationship between these mineralization types, but initial geochronological results outlined below support a sufficiently short time frame to allow a genetic link between the mineralization types.

Although the principal Au-bearing vein systems in the Wells-Barkerville area are commonly concentrated near, and are kinematically compatible with formation during dextral displacement along north-trending faults, this relationship does not explain the stratabound nature of the vein systems, which instead also suggests a significant element of control by northwest-trending structures. Northeast-dipping S_2 foliation-parallel slip surfaces and high-strain zones are common in the underground workings, often attenuating fold limbs, and may have been active up until late during D_2. If so, as a northwest-trending corridor of higher strain, these could represent the principal fluid channels to the Au-bearing veins, which if still active into waning stages of D_2 when northerly trending faults formed, then intersecting thrust surfaces with the faults may have created structurally permeable sites for fluid focus and vein deposition. If northeast-dipping, late-D_2 thrust corridors control vein mineralization, then this may explain the association with earlier replacement mineralization if it too formed earlier along the same D_2 high-strain corridors.

Wells-Barkerville Area: Dating and Isotopic Studies

Field studies in the Wells-Barkerville area during 2008 included the re-examination of key rock units and styles of mineralization in outcrop and drillcore, and extensive sampling for $^{40}Ar/^{39}Ar$ and U-Pb zircon dating and sulphide Pb isotope studies. A total of thirteen $^{40}Ar/^{39}Ar$ ages for micas have been determined from throughout the Wells-Barkerville area, using samples previously collected by Rhys and Ross (2001) when underground workings were still accessible, allowing access to areas of historic mining. New dating results are presented in Table 1.

The better-constrained $^{40}Ar/^{39}Ar$ results define a relatively narrow age range, from 138.2 to 155.2 Ma, for samples of country rock schist, micaceous alteration zones around known Au deposits and mica samples in and adjacent to

Table 1. Summary of new $^{40}Ar/^{39}Ar$ dating results from Wells-Barkerville area.

Sample No.	Rock Type and Location	Interpreted $^{40}Ar/^{39}Ar$ Age
BL-073	Baker unit, sericitic quartzite, Lowhee Creek	Rising spectrum to ca. 153 Ma (re-run rising spectrum to ca. 150 Ma)
BL-135	Rainbow 2 unit (upper) 1500 Level Cariboo Gold Quartz mine; muscovite-quartz-carbonate phyllite	146.6 ± 1.1 Ma (poor plateau)
BL-122A	Deformed pre-mineral vein, 1200 Level Cariboo Gold Quartz mine; muscovite coating fractures and in vein envelopes	153.7 ± 0.9 Ma (good plateau)
BL-130	Deformed pre-mineral vein, from Myrtle prospect trenches	155.2 ± 1.0 Ma (excellent plateau)
BL-086	Baker unit, north Lowhee Creek, muscovite-quartz phyllite in hanging wall of Bonanza Ledge zone	151.5 ± 0.8 Ma (good plateau)
BL-043	Fuchsite bearing Fe-carbonate, muscovite alteration of calcareous mudstone along Lowhee Creek	151.5 ± 0.8 Ma (excellent plateau)
BL-133-4	4400 Level Mosquito Creek Mine; banded fine grained ankerite-pyrite replacement ore	148.5 ± 1.0 Ma (excellent plateau)
2K-31, 211-1	Replacement ore, Bonanza Ledge zone; banded muscovite-pyrite phyllite with coarse pyrite-Fe-carbonate bands	138.2 ± 0.8 Ma (good plateau)
BL-134-1	Replacement ore, Bonanza Ledge zone; muscovite phyllite with disseminated pyrite	Rising spectra to ca. 142 Ma (re-run 135.5 ± 0.8 Ma; partial plateau)
BL-002	Muscovite phyllite with oxidized pyrite porphyroblasts in hangingwall of Bonanza Ledge zone	142.8 ± 0.8 Ma (good plateau)
BL-125-1	Diagonal quartz vein, 1200 Level Cariboo Gold Quartz mine; clots of coarse randomly oriented muscovite within vein	147.6 ± 0.8 Ma (good plateau)
BL-129-1	Extensional quartz vein, 4400 Level northwest of Mosquito Creek mine; coarse muscovite on envelope to vein	141.4 ± 0.8 Ma (excellent plateau)
BL-128-1	Extensional quartz vein, 4400 Level southwest of Mosquito Creek mine; randomly oriented coarse muscovite	142.6 ± 0.8 Ma (excellent plateau)

both early (deformed) and late quartz veins. Muscovite in hostrock schist and associated with early, deformed quartz veins tend to give slightly older ages (>146.6 Ma), whereas muscovite from within replacement style and extensional-vein style Au ore gives largely overlapping ages in the range of 138.5–147.6 Ma. The Wells-Barkerville area has only experienced metamorphism up to lower-greenschist facies (sub-biotite isograd) and peak metamorphic temperatures (and growth or recrystallization of muscovite) were associated with the earlier stages of deformation (D_1 and D_2; Struik, 1988; Schiarizza and Ferri, 2003; Ferri and Schiarizza, 2006). Peak temperatures of metamorphism in the area, therefore, did not exceed 400–430ºC and may have been somewhat lower. Since the closure temperature of the Ar isotopic system in muscovite is ~350ºC, it is suggested that the $^{40}Ar/^{39}Ar$ muscovite ages listed above are probably close to the age of formation and do not reflect slow cooling of the Barkerville terrane as a whole. If correct, this would suggest that the last significant metamorphic event that affected the region associated with the D_2 event occurred in Late Jurassic to earliest Cretaceous time, and most or all of the Au mineralization in the Wells-Barkerville area formed at approximately the same time or very slightly later. Such timing is feasible, given the field relationships described above. Four additional muscovite samples from occurrences within the Wells-Barkerville area are currently being dated using $^{40}Ar/^{39}Ar$ methods, along with biotite from a late lamprophyre dike.

Andrew et al. (1983) reported Pb isotopic analyses for galena from four Au-bearing quartz veins and one replacement-style sulphide occurrence in the Wells-Barkerville area and areas farther to the south. An additional three galena and six pyrite samples from veins and two pyrite samples from replacement-style mineralization have been analyzed from the Wells-Barkerville area (mainly Mosquito Creek and Bonanza Ledge zones). The combined datasets are shown in Figure 7, along with the 'shale curve' of Godwin and Sinclair (1982) for reference.

All of the sulphide Pb isotopic analyses for the Wells-Barkerville area and vicinity fall on or above the 'shale curve', which is an approximation of the evolution of Pb isotopes within both the North American miogeocline in the northern Cordillera and the pericratonic terranes that lie immediately to the west (including the Barkerville terrane). This indicates that the Pb and presumably all other contained metals in the deposits and occurrences in the Wells-Barkerville area are entirely of crustal derivation, and could potentially have been derived from local bedrock units. In addition, analyses of sulphide minerals from replacement-style mineralization completely overlap with those from crosscutting quartz veins, suggesting that the metals in these two distinct styles of mineralization had very similar sources and the veins and replacements are very similar in age (as also suggested by the $^{40}Ar/^{39}Ar$ dating results discussed above). A total of 23 additional sulphide samples, representative of the complete range of styles and geographic location of Au occurrences within the Wells-Barkerville area and vicinity, are currently being analyzed.

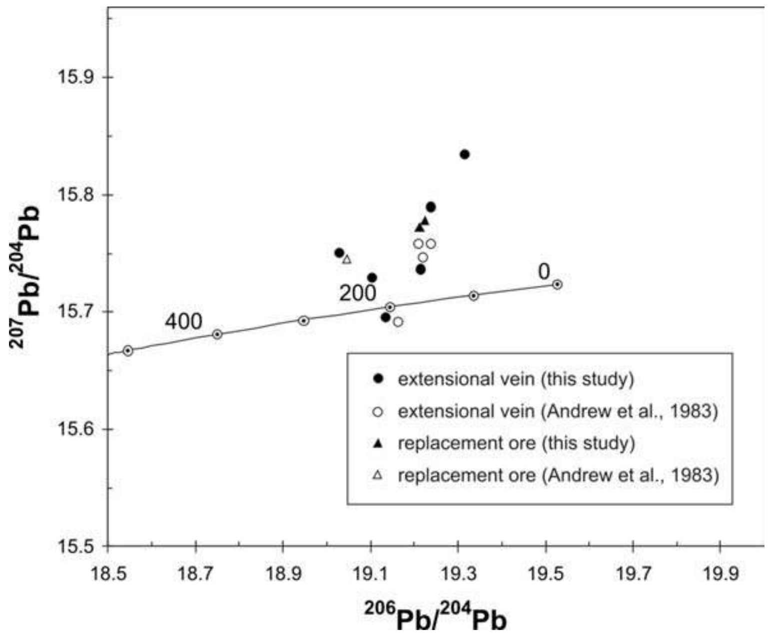

Figure 7. Sulphide Pb isotopic compositions from replacement- and vein-style Au mineralization in the Wells-Barkerville area. The 'shale curve' of Godwin and Sinclair (1982) is shown for reference.

Cunningham Creek Area

Southeast of the Wells-Barkerville area, vein showings extend discontinuously over a 40 km strike length to Cariboo Lake, and are associated with significant placer-Au–producing drainages such as Cunningham, Keithley, Antler and Grouse creeks (Schiarizza, 2004). These collectively define the southern portion of the eastern mineralizing trend in the Barkerville terrane illustrated in Figure 1. This area, and the Yanks Peak area to the west, were both visited during the fieldwork program to assess mineralization controls and collect geochronological and isotopic samples. Initial observations from the Cunningham Creek work are summarized here for comparative purposes to the nearby Wells-Barkerville area. Geochronological and isotopic analyses are underway.

Gold prospects along Cunningham Creek (Figure 1) include the Craze Creek, Hibernian, B zone, Jewelry Shop, Silver Vein and Cariboo Hudson (093A 071) prospects. Within these areas, lode-Au mineralization occurs mainly in sets of structurally late quartz-sulphide veins of comparable style to those at the Wells-Barkerville area, although the controls by north-trending faults are more apparent, and veins more frequently display a semibrittle style. The hostrock type is a northwest-trending grey phyllite of the Downey succession (Schiarizza and Ferri, 2003).

In the vicinity of Craze Creek, three prospects (Hibernian, Jewelry Shop and the B zone) comprise at least three north-trending, mineralized fault zones in which fringing arrays of Au-bearing quartz-sulphide veins are developed. The faults comprise narrow, semibrittle shear zones that trend north with steep dips, and cut across the northwest-trending, moderately northeast-dipping phyllite sequence. Primary compositional layering, dominant foliations (S_1 and S_2) and deformed quartz veins locally deflect into parallelism with more northerly trends as they approach the shear zone slip surfaces (Figure 8a), which with offset lithological contacts and synthetic shear bands record dominantly dextral displacement on the fault-slip surfaces. Gold-bearing quartz veins, often with coarse-grained pyrite-arsenopyrite and minor galena and sphalerite fill are abundant within several metres of, and between closely spaced slip surfaces (Termuende, 1990). The larger veins, which are up to 1 m thick, trend northwest, exploiting S_1 foliation surfaces, but rapidly thin within a few metres of the shear-zone slip surfaces. Extensional veins and veinlets rotate from east-west to west-northwest trends as they approach slip surfaces, defining sigmoidal geometries both consistent with the shear sense, and with vein formation simultaneous with dextral displacement on the shear zones. Minor sigmoidal dextral extensional vein arrays are present adjacent to the shear zones, recording similar kinematics (Figure 8b).

To the south of the Craze Creek prospects, prospects including Skarn (Silver mine), Penny Creek and Cariboo Hudson comprise northerly to north-northwesterly trending, discordant and steeply dipping fault-fill veins (Delancey, 1988; Termuende, 1990). Deflections of rock units and foliations, as well as offsets of lithological contacts by a few metres to tens of metres, record dextral displacement across the veins, consistent in shear sense to the shear zones at Craze Creek. These veins contain abundant galena, sphalerite, pyrite, tetrahedrite and arsenopyrite, which may be banded parallel to vein walls (Figure 8c). The veins are much more Ag-rich than those in the Craze Creek area to the northwest. Collectively, these define a corridor of mineralized faults and veins that is approximately 600 m wide along the east side of Cunningham Creek.

a)

b)

c)

Figure 8: Vein systems in the Cunningham Creek area: **a)** plan view of north-trending, quartz-vein–filled shear-zone slip surface (at centre, runs from left to right) that truncates the adjacent grey pyrite-arsenopyrite-quartz veins at the Jewelry Box showing; the veins emanate off the slip surface and are parallel to northwest-trending S_1 foliation; note deflection of the deformed quartz veins and S_1 foliation into the shear plane at the centre, compatible with dextral displacement along the structure; hammer for scale; **b)** northeast-trending sigmoidal en échelon array of extensional veins adjacent to the Jewelry Box shear zone records dextral shear; hammer for scale; **c)** view northward of the Silver Vein occurrence; this is a north-trending, steeply east-dipping banded shear vein that is fault hosted and contains quartz, pyrite, galena and tetrahedrite; deflection of S_1 foliation and juxtaposition of quartzite (right) against carbonaceous phyllite (left) across the fault and vein suggest dextral displacement; person for scale.

The Cunningham Creek area veins display similar timing relationships to regional fabrics such as main-stage, Au-bearing quartz veins in the Wells-Barkerville area. The veins postdate all D_1 and most or all D_2 strain, and are associated with northerly trending dextral faults. The style of associated shear zones at Craze Creek is more semibrittle in character than is generally seen in the Wells-Barkerville area or other areas, potentially suggesting slightly higher temperatures or lower strain rates during vein formation. The veins are also kinematically consistent with formation in response to northeast-directed shortening, potentially late during D_2. As in the Wells-Barkerville area, despite being hosted by discordant northerly trending fault and shear zones, mineralization is generally stratabound and is localized principally in the northwest-trending package of the Downey phyllite within several hundred metres of the contact with black siltite and phyllite of the Hardscrabble succession (Schiarizza and Ferri, 2003).

Geological Setting and Au Mineralization in Quesnellia Metasedimentary Units

Two significant Au deposits have been discovered within lower-greenschist–grade metasedimentary and metavolcanic units in the lower part of Quesnellia: these are the Spanish Mountain (CPW) deposit, which is held by Skygold Ventures Ltd., and the Frasergold deposit, which is currently being evaluated by Hawthorne Gold Corp. (Figure 1).

Spanish Mountain (093A 043)

The Spanish Mountain deposit occurs within the black phyllite package of the Quesnel terrane, approximately 3 km east of its probable thrust contact with overlying mafic volcanic rocks of the Nicola Group to the southwest (Spanish thrust, Figure 1; Logan, 2008). The deposit is hosted by interbedded slaty to phyllitic, dark grey to black siltstone, carbonaceous mudstone, greywacke and minor conglomerate that are locally intruded by plagioclase±quartz–phyric dikes and sills.

Rocks in the vicinity of the Spanish Mountain deposit are folded, but generally trend northwest with overall northeasterly dips. Graded bedding in drillholes observed suggests that the sequence is in an overturned, megascopic F_1 fold limb (Singh, 2008). Previous work by Skygold Ventures (Singh, 2008) and surface mapping and drillcore review conducted during this study have established that the stratigraphy in the deposit area comprises two main lithological packages:

An extensive lower package of siltstone and fine-grained greywacke that underlies southwestern portions of the ridge crest of Spanish Mountain southwest of the main zones of the deposit and forms the structurally lowest, but stratigraphically highest part of the immediate lithological sequence of the deposit.

A sequence of carbonaceous phyllite and interbedded siltstone that structurally overlays the siltstone-greywacke sequence to the northeast and contains two prominent marker units: a fine-grained, pale-grey greywacke unit (typically 40–100 m thick) that contains a heterolithic and mud-chip conglomerate marker (<1–10 m thick) at its base, and a siltstone unit (70–130 m in thickness) that is often silicified and carbonate-sericite–altered, and contains altered, thin sills of probable mafic protolith. This sequence of dominantly carbonaceous phyllite is the principal host to mineralization at the deposit. It has been further subdivided into three units based on their stratigraphic position with respect to the markers termed from structurally lowest (in the southwest) to highest (in the northeast): the Lower, Main zone and North zone argillites (Singh, 2008). Volumetrically

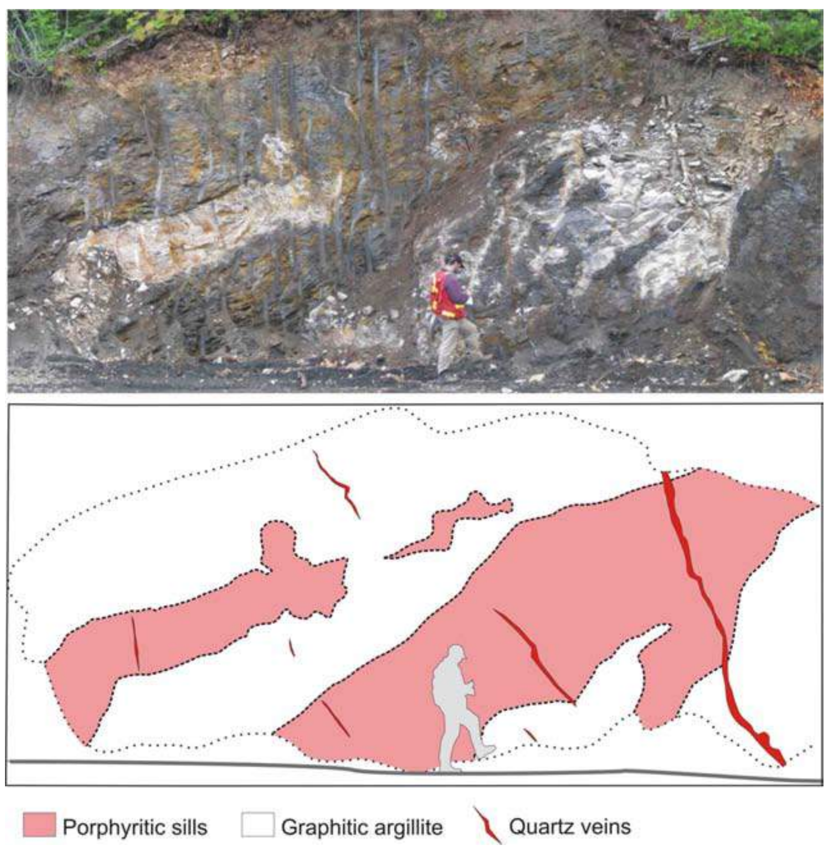

Figure 9: View to the southwest of a drill cut-out in lower portions of the carbonaceous phyllite sequence on Spanish Mountain. The photo illustrates two concordant, deformed and S_1-parallel porphyritic sills (in pink in the schematic diagram) that are cut by northwest-trending, steeply northwest-dipping quartz extensional veins (shown in red). These intrusions have yielded U-Pb zircon ages of 185.6 ±1.5 to 187 ±0.8 Ma.

minor amounts of interlayered mafic tuff and amygdaloidal basalt also occur within the sequence outside of the immediate deposit area (Singh, 2008).

The Spanish Mountain sequence is also characterized by the presence of plagioclase±quartz±hornblende sills and locally dikes, which commonly occur in the Lower argillite at the structural base of the carbonaceous phyllite sequence (Figure 9). They are also present in the siltstone-greywacke sequence to the southwest on the top of the ridge. The sills range in thickness from a few tens of centimetres to locally up to 100 m thick, the latter in one lenticular sill at the contact between the carbonaceous phyllite and underlying siltstone and greywacke sequences southwest of the deposit. These sills are affected by all phases of folding, alteration and quartz-vein mineralization (Figure 9). Locally irregular outlines to the contacts of these sills and brecciation on their finer-grained margins that may represent peperitic textures suggest that they may have been intruded into unconsolidated sediments. Variable proportions of quartz, feldspar and porphyritic textures suggest a suite of different intrusions. Probable mafic sills that are present within the altered siltstone marker unit are generally narrow and may be laterally discontinuous, locally becoming discordant to S_0.

Alteration

Widespread alteration affects rock types on Spanish Mountain. The most extensive alteration consists of iron-magnesium-carbonate+muscovite (sericite)±pyrite with accessory rutile that varies in style between different rock types. Two generations of carbonate occur as discrete porphyroblasts in the finer-grained carbonaceous phyllite and silty units; an early phase with rounded porphyroblasts up to 0.8 cm in diameter, which is wrapped by the dominant foliation, displaying a 'knotted' texture and a younger phase of rhombic porphyroblasts that overgrows at least the S_1 foliation. In the greywacke and the feldspar-porphyry sills, carbonate-sericite alteration is finer grained, more pervasive and commonly texturally destructive, which in some cases hinders distinction between the two rock types. The alteration does not affect carbonaceous material in the carbonaceous phyllite, which remains dark in colour. Altered greywacke and feldspar-phyric intrusions are pale tan to nearly white. Locally, in the greywacke marker of the upper sequence and in quartz-bearing intrusive phases, fuchsite occurs as mantles around isolated, probable xenocrysts of chromite and small angular mafic or ultramafic xenoliths. The most intense alteration affects the siltstone marker that lies between the Main and Upper argillite units in the upper carbonaceous phyllite sequence, and the structurally lower portions of the greywacke marker unit. The siltstone marker package is intensely carbonate-sericite–altered, bleached and silicified, and textural evidence suggests that siltstone may have been hornfelsed (quartz-biotite altered), possibly related to the intrusion of mafic sills, prior to the bleaching, which is related to the carbonate-muscovite alteration. In this unit, bright green chrome mica (fuchsite), intergrown with intense carbonate alteration assemblages, replaces the mafic sills that cut the silicified siltstone package. Pervasive alteration of the types described above predate at least S_2 foliation, since muscovite is aligned within foliation planes, fuchsite may occur as S_2-parallel stylolitic pressure-solution seams, and carbonate porphyroblasts are often wrapped by dominant foliation.

Structural History

The sequence of deformation in the Spanish Mountain area is consistent with the general phase 1–phase 2 events defined by Bloodgood (1992) and Panteleyev et al. (1996) for the region, although local differences in fold geometry and an additional folding event that differ from these previous interpretations are also evident. First-phase (S_1) foliation is generally layer parallel and penetrative. Isoclinal F_1 fold hinges were locally observed in the greywacke marker unit, where they are likely intrafolial and may result in local tectonic thickening of some units. Presence of dominantly overturned bedding facing directions in drillholes in the deposit area suggest that the hosting lithological sequence is inverted (Singh, 2008). This implies that the deposit may lie on the overturned limb of an F_1 fold nappe, a geometry that has not been previously documented in this part of the Quesnel terrane.

Second-phase foliation development at Spanish Mountain comprises moderate to shallow southwest-dipping spaced foliation that is axial planar to the folds, crenulates and locally transposes S_1, and is axial planar to dominant, northeasterly verging phase 2 folds. Fold axes plunge shallowly southeast. Map patterns and cross-sectional interpretation suggest that a megascopic, recumbent phase 2 fold hinge with a broad hinge zone lies in the northeast portions of the deposit area, separating the sequence into moderately northeast dipping and subvertical limbs to the southwest and northeast, respectively, on the northern flanks of Spanish Mountain in the vicinity of the North zone. At a property scale, phase 2 fold hinges may be noncylindrical and vary in plunge direction (B. Singh, pers. comm., 2008), potentially due to interaction with previous phases of folding.

A significant observation from the current study is that an additional phase of folding is evident in the Spanish Mountain area between the regional phase 1 and phase 2 events of Panteleyev et al. (1996). These open to tight folds affect S_1 foliation but are obliquely crossed and overprinted by the spaced, second-phase foliation. Folds of this type plunge moderately to the southeast, and have steeply dipping axial planes; axial-planar cleavage is weakly developed or absent. These folds are best developed and widespread in the siltstone-sandstone unit southwest of the main deposit area, but also occur locally in the higher carbonaceous phyllite sequence where they were observed to affect portions of the silicified siltstone unit. For the purposes of this paper, they are coded F_{2a} folds, whereas the folds and foliation associated with the widespread second-phase foliation are coded F_{2b} and S_2, respectively, for consistency with the defined regional nomenclature. The megascopic phase 2 fold (F_{2b}) mentioned above is likely accentuated by, and may tighten earlier folds associated with this additional F_{2a} event. The presence of these folds suggests that the regional structural history may be more complex than has been previously determined, although telescoping of subsequent events may obscure such patterns.

As in other parts of the district, latest prominent structural features in the Spanish Mountain area comprise north- to northeast-trending brittle faults. Faults measured during this study most frequently have moderate to steep west-northwest dips and north-northeast trends. Significant northwest-trending faults were also observed locally. The faults are typically defined by zones of clay gouge, which

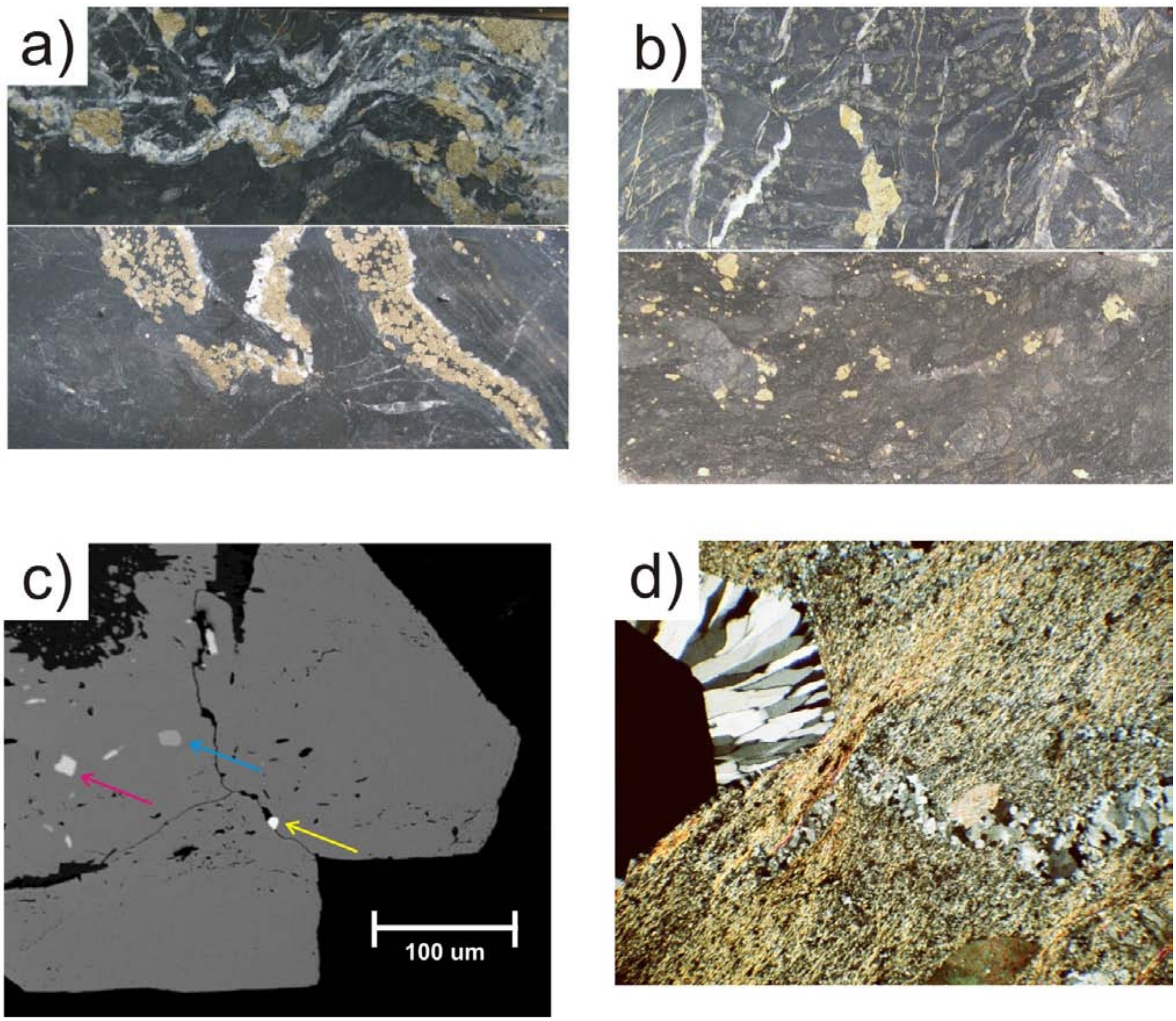

Figure 10: Early pyrite-quartz veinlets and disseminated pyrite in carbonaceous phyllite, Spanish Mountain deposit: **a)** folded quartz-pyrite veinlets; note fine- to medium-grained habit of pyrite and euhedral nature of the pyrite grains in the lower sample; (top) DDH515, 102.9 m; (bottom) DDH697, 155.5 m; both of these samples contained <1 g/t Au; **b)** (top) pyrite-quartz stringers at high angle to S_0 in thinly laminated phyllite are affected by incipient ptygmatic folding; pyrite is euhedral; DDH259, 57.0 m, from interval grading 2.22 g/t Au; (bottom) disseminated pyrite±quartz aggregates in tectonically disrupted carbonaceous mudstone; DDH289, 21.0 m, 3.13 g/t Au; **c)** scanning electron microscope (SEM) backscatter image of euhedral pyrite aggregate from sample in b) (bottom); note mica trails inside the pyrite that defines S_1 foliation, indicating pyrite formation after D_1; a grain of electrum (yellow arrow) occurs on a fracture between pyrite grains, while chalcopyrite (red arrow) and sphalerite (blue arrow) are encapsulated in the pyrite; 'um' = microns; **d)** photomicrography illustrating a quartz pressure shadow on a euhedral pyrite grain (opaque, at left); fibres in the pressure shadow are aligned parallel to the S_2 foliation defined by sericite in the surrounding phyllite; note folded quartz veinlet at right; DDH252, 116.7 m, in an interval grading 3.46 g/t Au; plane-polarized light, field of view 3 mm.

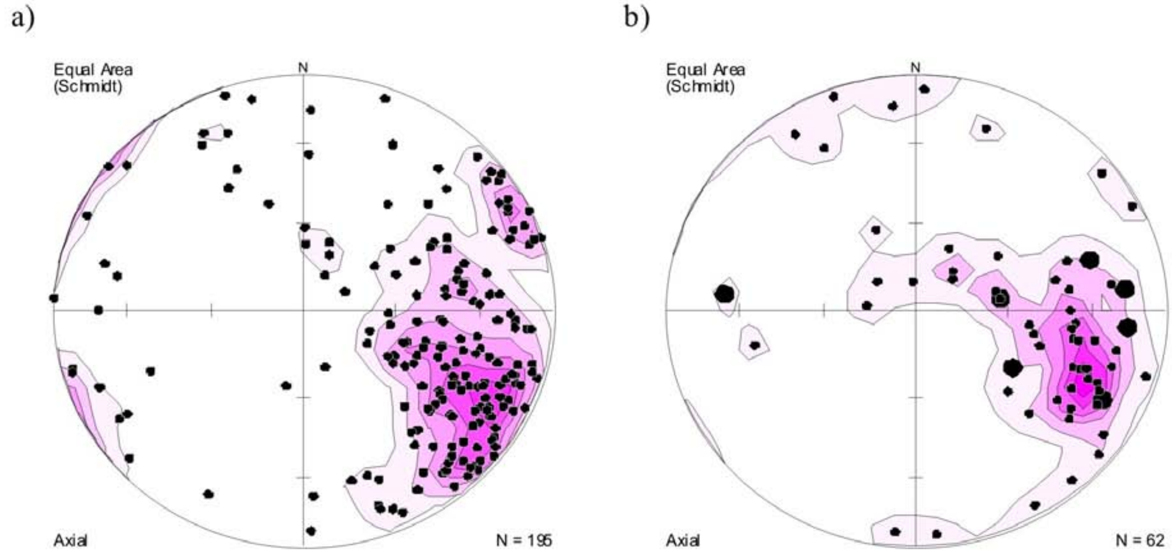

Figure 11: Equal-area projections of poles to orientations of quartz veins in the Spanish Mountain deposit. All data were collected by the authors in 2008: **a)** quartz veins <5 cm thick; these are dominantly extensional veins; steep northwest dips predominate, but veins also range to more northerly and northwesterly trends with west to southwest dips; **b)** quartz veins >5 cm thick, including fault-hosted and shear veins; note the dominant northerly trends and steep westerly dips, which include several significant faults containing cataclastically deformed vein material; large dots represent ribboned shear veins, mainly from the North zone.

commonly include cataclastically deformed quartz-vein material. These, however, may in part be localized along earlier, probably more semibrittle shear zones since it was noted, particularly in drillcore, that foliated chloritic or more intensely foliated shear zones and foliated cataclasite were commonly present, and localized some quartz veining. Fault thickness is highly variable, with thicker faults containing up to several metres of gouge and broad damage zones. Carbonaceous material has in some cases been remobilized along fractures and veinlets into carbon-poor greywacke and intrusions, locally forming black crackle breccia adjacent to faults and larger associated quartz veins.

Gold Mineralization

The Spanish Mountain deposit is a bulk tonnage Au system that also includes local higher-grade Au-bearing quartz veins. The most economically significant Au mineralization (>1 g/t Au) occurs in wide zones (10–135 m) hosted dominantly within the black argillite and siltstone, and to a lesser extent in greywacke, often straddling the contact (Singh, 2008). These zones may occur as a set of stacked, roughly lensoidal zones, which at a local scale are stratabound and spread most widely along carbonaceous phyllite ('argillite') units, but at a deposit scale are stacked and linked, defining an overall northerly elongate mineralizing system that is developed discordantly across several stratigraphic horizons. The largest zone identified to date is the 'Main zone', which has been traced by drilling over a strike length of approximately 1.3 km and width of 500 m (Singh, 2008). The 'Lower zone' occurs beneath the Main zone, in the structurally lower, carbonaceous argillite unit of the same name. The smaller, less well-defined North zone occurs in the structurally highest carbonaceous unit (Singh, 2008).

Within these mineralized zones, there are at least two periods of mineralization: an earlier phase of disseminated pyrite and pyrite-quartz veinlets, and a later phase of fault-related quartz veining. The early pyrite mineralization comprises stringers and up to 2 cm wide veinlets of pyrite+quartz+iron-magnesium-carbonate and spatially associated disseminated pyrite that are preferentially developed within carbonaceous phyllite in mineralized zones (Figure 10a, b). The disseminated pyrite often occurs in aggregates with quartz. Pyrite in both the veinlets and disseminations varies from fine to medium grained and is often euhedral. Carbonaceous phyllite may be tectonically disrupted, with destruction of S_1 foliation and incipient cataclastic brecciation in areas of pyrite development (Figure 10b), and veinlets and pyrite may occur on or adjacent to slip surfaces that define narrow shear zones, suggesting potential control by faulting, possibly thrust faults, along the carbonaceous (graphitic) argillite units. Pyrite-quartz veinlets are often ptygmatically folded and are affected by at least D_2 strain (Figure 10a). The euhedral disseminated pyrite grains and aggregates overgrow S_1 foliation and early folds, which may be preserved as micaceous trails within the grains (Figure 10c), but in turn are wrapped by S_2 foliation and have fibrous quartz pressure shadows aligned parallel to S_2 surfaces (Figure 10d), collectively suggesting that they formed late during or after D_1, and prior to most D_{2b} strain. Electrum and native gold have been observed as <5–20 m grains encapsulated in and along fractures in this

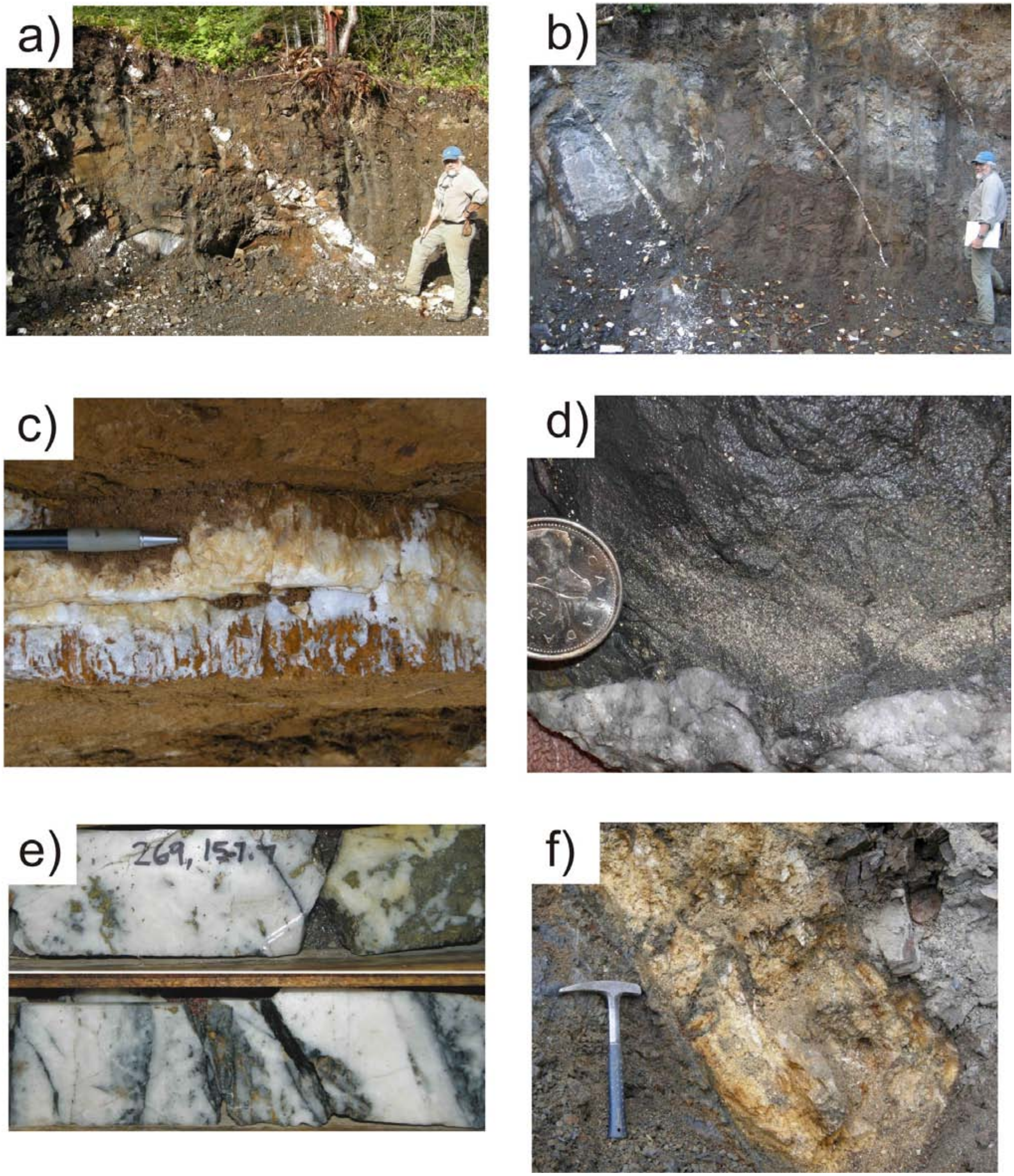

Figure 12: Spanish Mountain Au-bearing quartz veins: **a)** sheeted northwest-dipping quartz extensional veins hosted by carbonaceous phyllite in the North zone surface exposures, view southwest, person for scale; **b)** sheeted northwest-dipping quartz extensional veins hosted by carbonaceous phyllite in the Main zone surface exposures, view southwest, person for scale; **c)** extensional vein in sill hosted by the southern siltstone sequence shows paragenesis from early fibrous quartz-carbonate on margins, to more massive quartz-pyrite in core, pencil for scale; **d)** M1 pit, quartz extensional vein (below) with pyrite envelope (centre) in carbonaceous phyllite, quarter for scale; **e)** brecciated, friable rusty quartz vein in northerly trending, west-dipping fault; view south, Main zone exposures; core is approximately 5 cm wide; **f)** high-grade (23.9 g/t Au) ribboned quartz shear vein with pyrite clots (above) and carbonaceous-pyritic black slip surfaces and breccia bands (below) in a fault zone; hole 269, 157.7 m; hammer for scale.

style of pyrite and free in the quartz carbonate within the veinlets (Ross, 2006), indicating that this early pyrite-quartz episode introduced Au into the system, where it may contain a significant amount of low-grade mineralization in the deposit (Singh, 2008). Although it is possible that some of the euhedral pyrite could have formed from recrystallization or remobilization of an earlier, potentially Au-bearing diagenetic or synsedimentary pyrite phase (that has locally been identified at Spanish Mountain; R. Large, pers. comm., 2007), the common association of the euhedral pyrite with quartz veinlets, occurrence of pyritic zones as multiple stacked zones that occur across different stratigraphic horizons, lateral decreases in pyrite abundance in stratigraphic units away from mineralized zones, and local cataclastic brecciation of carbonaceous phyllite in pyritic areas suggests that the pyrite is dominantly hydrothermally and tectonically controlled. Although this style of mineralization is clearly auriferous in many areas, no direct correlation between Au grade and pyrite content has been established (Singh, 2008).

The second mineralizing event at Spanish Mountain is associated with tectonically late quartz veins and faults that share similarities with the dominant, late vein-related Au mineralization episode in the Barkerville terrane. They cut the folded, early quartz-pyrite veins described above and are most often manifested by sets of sheeted, northeast-trending and steeply northwest-dipping (Figures 11a, 12a, b) quartz±iron-carbonate extensional veins <5 cm thick that may contain minor pyrite, galena, sphalerite and tetrahedrite. In surface exposures, base metals were noted most abundantly in veins within the North zone. Sheeted extensional veins are typically spaced from a metre to several metres apart in mineralized carbonaceous phyllite (Figure 12a, b). Vein densities are often much higher in sandstone and in feldspar- or quartz-phyric sills. While usually having blocky quartz fill, prismatic quartz and fibrous quartz-carbonate aligned at high angles to vein walls are also often present, consistent with an extensional origin. A paragenesis of early quartz-carbonate on vein margins and central blocky quartz vein fill is locally apparent, and similar to vein paragenesis observed in the Wells-Barkerville area (Figures 4b, 12c). Locally, more than one generation of veining is developed, with successive generations becoming less carbonate rich and more quartz rich, consistent with the paragenesis described above (B. Singh, pers. comm., 2008). The extensional veins may have disseminated pyrite envelopes that extend for several centimetres into the surrounding wallrock (Figure 12d).

In drillcore, areas of highest Au grade and most occurrences of visible Au were associated with quartz veins. Gold grades typically increase in areas of quartz veining, particularly in association with mineralized faults (*see* below), although a direct association between quartz vein density and grade has not been established (Singh, 2008). It was noted, however, that quartz-vein distribution in outcrop mimics that of the distribution of mineralized zones. To the south in the lower siltstone package, Au prospects (e.g., Ropes of Gold) occur principally in folded plagioclase-phyric sills where they are cut by sets of quartz extensional veins, which often have pyrite envelopes.

Extensional veins are also associated with shear veins and fault-hosted veins. North-northeast-trending, west-northwest-dipping (Figure 11b) clay gouge-filled faults, commonly containing unconsolidated, cataclastically deformed vein material (Figure 12e), are present within many outcrop exposures, and are often intersected in drillcore in mineralized zones. These may be surrounded by more concentrated sets of extensional veins, which were in several cases noted to join the fault-hosted veins suggesting a coeval timing. Several fault-hosted shear veins up to 2 m thick were also noted in core and outcrop, comprising ribboned quartz-pyrite veins with carbonaceous or pyritic stylolitic slip surfaces and banding (Figure 12f), and which have been variably brecciated by later, postmineralization brittle displacement. These locally contain high Au grades.

Since significant postmineralization faulting has occurred along the faults hosting vein mineralization and has brecciated the quartz and obscured any primary kinematic indicators that may have been present, it is not possible to determine the syn-vein kinematics of faults. However, the association of steeply dipping, northeast-trending quartz extensional veins with the faults, and junction of some extensional veins with fault-fill veins, are geometrically compatible with the vein orientations in most portions of the Barkerville terrane, suggesting syn-vein dextral oblique slip (northwest side down) faulting in response to northeast-directed shortening. The structurally late timing of extensional veins at Spanish Mountain, which cut across all fabrics and folds without deflection, and the occurrence of extensional veining at high angles to the shallow southeast-plunging L_2 intersection lineation are also compatible with a late D_2 timing of vein formation.

Discussion

The proposed two-stage history of Au mineralization at the Spanish Mountain property may be analogous to the mineralizing history in the Wells-Barkerville area. As with that area, the later vein mineralization is spatially coincident with earlier forms of more deformed sulphide-bearing mineralization. It is unclear what the relative proportions of Au the early pyrite and later fault-related quartz-veining events each contribute at Spanish Mountain, but the later quartz-vein–associated mineralization is more widespread and often higher grade than the early pyritic mineralization. To explain the coincidence of the two forms of mineralization, simple remobilization of early mineralization during later events into the later quartz veins is considered unlikely here, as this process does not explain why vein quartz densities are highest in the mineralized zones. As with the Wells-Barkerville area, if remobilization was the main mechanism by which Au was localized into the later veins, the later veins themselves would be expected to be developed regionally, and not coincidentally focused in the older areas of mineralization. The occurrence of both the early mineralization and quartz veining in a series of stacked zones that collectively cross stratigraphic boundaries in a crudely northerly elongate zone with evidence for cataclasis and faulting associated with both the early and later mineralizing episodes suggest that the Spanish Mountain deposit may be developed in a zone of longer-lived tectonic activity. Widespread early alteration of the Spanish Mountain sequence near mineralized zones in the form of carbonate porphyroblast development, sericite-carbonate alteration of feldspathic rock types, and fuchsite-carbonate alteration of mafic sills in the silicified siltstone marker may be coincident with the earlier pyrite-quartz event, as these styles of alteration are affected by D_{2b} fabric. Early, local silicification of the siltstone marker, potentially associated with the mafic sills, may have also aided in fluid focus and vein development during the later quartz-veining events, by forming an impermeably and rheologically competent buttress to fluid flow.

Ongoing Dating, Petrographic and Isotopic Studies at Spanish Mountain

During the fieldwork at Spanish Mountain, an extensive suite of samples for $^{40}Ar/^{39}Ar$ mica and U-Pb zircon dating, as well as for detailed petrographic, lithogeochemical and Pb isotopic studies were collected, and analyses are currently underway. A lithogeochemical study of the intrusive rocks is also currently in progress.

Zircon grains have been separated from four separate intrusive bodies that intrude the contact area between the lower siltstone and upper carbonaceous phyllite sequence at Spanish Mountain. These have recently been dated at the University of British Columbia (UBC) using laser ablation inductively coupled plasma–mass spectrometry (ICP-MS) U-Pb methods. The four samples give similar ages of 185.6 ±1.5 Ma to 187.3 ±0.8 Ma. These intrusions have been affected by D_1 deformation and later events, having been boudinaged and wrapped by S_1 foliation. Consequently, these ages place a maximum age on both the D_1 deformation that has affected the phyllite in this area and the Au mineralization and associated alteration. These intrusions may be related to the suite of Jurassic-aged intrusions (unit 7 of Panteleyev et. al., 1996), which are mapped as isolated stocks in the same sedimentary package of rocks to the south of Quesnel and Horsefly lakes, and to the west where they intrude the Triassic–Early Jurassic basaltic rocks and related volcaniclastic rocks. The only dated bodies in the unit 7 suite, however, have given somewhat older ages (>193 Ma) and compositionally, these bodies most closely resemble those in the Mt. Polley area, all of which have been dated at ca. 200 Ma using U-Pb methods (Mortensen et al., 1995). The only intrusions within Quesnellia that have given reliable (U-Pb) crystallization ages similar to those in the Spanish Mountain area are those that are associated with the Mt. Milligan Cu-Au porphyry system north of Prince George.

Frasergold (093A 150)

The Frasergold property, located approximately 60 km southeast of Spanish Mountain, covers an ~10 km long, northwest-trending area of mineralized prospects, defined by drilling and anomalous Au in soils along the northeast limb of the Eureka Peak syncline (Figure 1). Mineralization at Frasergold is hosted by the same general sequence of Middle–Upper Triassic metasedimentary rocks that occurs at Spanish Mountain, comprising a fine-grained turbidite sequence that is dominated by black carbonaceous phyllite with local thin interbeds of metasiltstone, and more rarely, fine-grained metasandstone. Unlike Spanish Mountain, however, intrusive rocks appear to be absent from the section at Frasergold. Stratigraphy in the Frasergold deposit area dips moderately to shallowly to the southwest in the deposit area. Regional mapping suggests that the overall sequence is upright and occurs on the northeast limb of the regional Eureka syncline (Bloodgood, 1987, 1992).

Alteration

The carbonaceous phyllite in the Frasergold deposit area, like portions of the Spanish Mountain sequence, is characterized by the presence of coarse iron-carbonate porphyroblasts. Foliation (both S_1 and S_2, *see* below) wraps around the porphyroblasts, creating a bumpy to dimpled 'knotted' texture to foliation surfaces. The porphyroblasts may represent a broad alteration envelope to the mineralizing system, as in other sediment-hosted districts globally. Although the carbonate porphyroblasts are wrapped by, and therefore predate S_2 foliation, they overgrow S_1 foliation surfaces and folds, indicating their formation during or after D_1, but prior to D_2 (Figure 13), and consistent with a secondary origin that could be alteration related. If they are related to mineralization, then this relationship helps constrain mineralization timing.

Gold Mineralization

Gold mineralization on the Frasergold property occurs within, or is spatially associated with stratabound sets of white quartz>iron-carbonate+muscovite+pyrite veins that are developed in the 'knotted' iron-carbonate porphyroblastic carbonaceous phyllite unit. The veins form complex sets that are developed in concentrated zones several metres to tens of metres wide that dip collectively to the southwest and form a bulk tonnage low-grade Au deposit. An inferred historical resource (not compliant with NI43-101) of 6.6 million tonnes grading 0.055 oz/t Au to depths of 100 m and over a 3 km strike length has been reported (Goodall and Campbell, 2007).

Structural History

Quartz veins within mineralized zones at Frasergold comprise mainly subparallel, approximately S_0/S_1 parallel (concordant) quartz veins and veinlets (Figure 14a) that are composed of blocky, recrystallized white quartz with minor iron-carbonate, and common silvery muscovite selvages. These veins are affected by both D_1 and D_2 strain and are often transposed and boudinaged in the plane of S_1, locally with the development of internal S_1-parallel sericite stylolite. The veins are affected by F_2 folds (Figure 14b) and vary in orientation across F_2 fold limbs, although are generally within or almost parallel with S_0/S_1. Yellow-brown, coarse, blocky iron-carbonate typically occurs as clots, bands and selvages on veins, and contains disseminated pyrite ±pyrrhotite with local trace amounts of chalcopyrite, sphalerite and galena.

The concordant S_0/S_1 and thicker, discordant veins join one another without crosscutting relationships (Figure 14c), have the same mineralogy, and are equally as deformed, suggesting that they are all part of a single vein generation, or several very closely timed but now indistinguishable vein generations that form part of a single veining episode. Although primary geometries and morphologies of the veins have now been obscured by deformation, the narrower concordant veins frequently form arrays with local en échelon patterns that splay off the larger discordant veins in a relationship that could represent a shear vein or extensional vein relationship, with the larger veins forming minor reverse oblique slip or shear veins (Figure 14c). The vein systems may have originally formed networks of widely spaced, reverse shear veins that were joined by sets of abundant extensional veins that could have been broadly localized along with, or adjacent to a thrust within the phyllite sequence. Collectively the vein networks, and potential stringer or disseminated pyrite mineralization in the vein wallrock, define a bulk-tonnage, low-grade deposit.

The Frasergold vein system could represent a semibrittle shear vein or extensional vein array that formed along with, or adjacent to a concordant or semiconcordant D_1 shear zone. Similar sets of veins associated with D_1 thrusts are reported throughout the region by Bloodgood (1992). An early to syn-D_1 timing of mineralization is suggested based on the strain state and relations of the veins to fabrics, since the veins are affected by a significant amount of D_1 strain, but predate all D_2 deformation. This is consistent with the late-D_1 to pre-D_2 implied timing of the carbonate porphyroblasts based on textural relationships. Apart from a few isolated stringers, structurally late, steeply dipping and northeast-trending quartz extensional veins and shear veins seen in the Barkerville lode-Au deposits and at Spanish Mountain are absent at Frasergold.

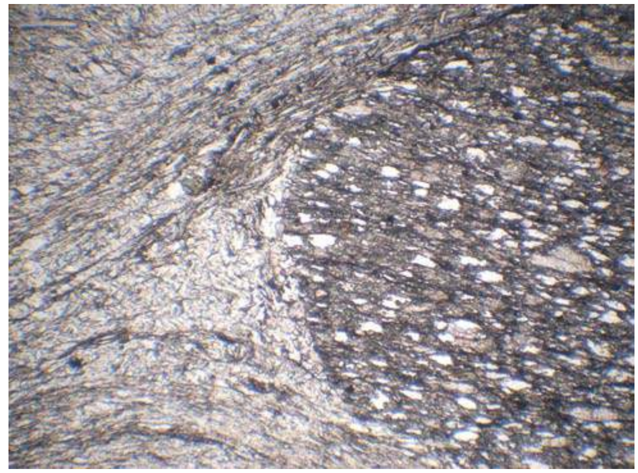

Figure 13: Photomicrograph of a carbonate porphyroblast (right side of image) in carbonaceous phyllite at the Frasergold deposit. Note the porphyroblast overgrows S_1 foliation, which is preserved as muscovite and quartz alignment internally within it. The S_2 foliation wraps around the porphyroblast at left and crenulates and transposes the older S_1 foliation outside the porphyroblast. Frasergold drillhole 07-295, 124.2 m. Plane-polarized light, field of view 3 mm.

Other Au occurrences of a similar style occur along strike to the southeast and northwest of the Frasergold deposit in the same belt of Triassic phyllite. The Kusk occurrence (093A 061; Belik, 1988) is located approximately 4 km south-southeast of Frasergold, and the Forks occurrence (093A 092; Howard, 1989) is just south of the east end of Horsefly Lake, approximately 20 km northwest of Frasergold. At both the Forks and Kusk occurrences, like the Frasergold deposit, Au occurs in variably deformed and boudinaged quartz veins within grey carbonaceous phyllite with iron-carbonate porphyroblasts. Collectively, these occurrences and the Frasergold deposit define a mineralized corridor that is nearly 35 km long.

Discussion

If the S_1 and S_2 fabrics at Frasergold can be convincingly demonstrated to be related across the CGD, then the Frasergold veins could be comparable to the early, deformed sets of pyrite-quartz veins observed at Spanish Mountain and the quartz-carbonate-muscovite veins that predate main phases of Au veining in the Wells-Barkerville area, which are also widespread in other lode-Au trends in the Barkerville terrane. Alternatively, if D_1 and D_2 deformation events and associated fabrics (S_1, S_2, L_2) that are recorded across the CGD are not coeval and instead are progressively transgressive across the area, the Frasergold mineralization may be coeval with other generations of veining, or potentially may represent a separate mineralizing event that is not manifested in other parts of the district. The former is considered most likely, since the Eureka Peak syncline and its associated fabrics can be traced continuously to the northwest to the Spanish Mountain area by

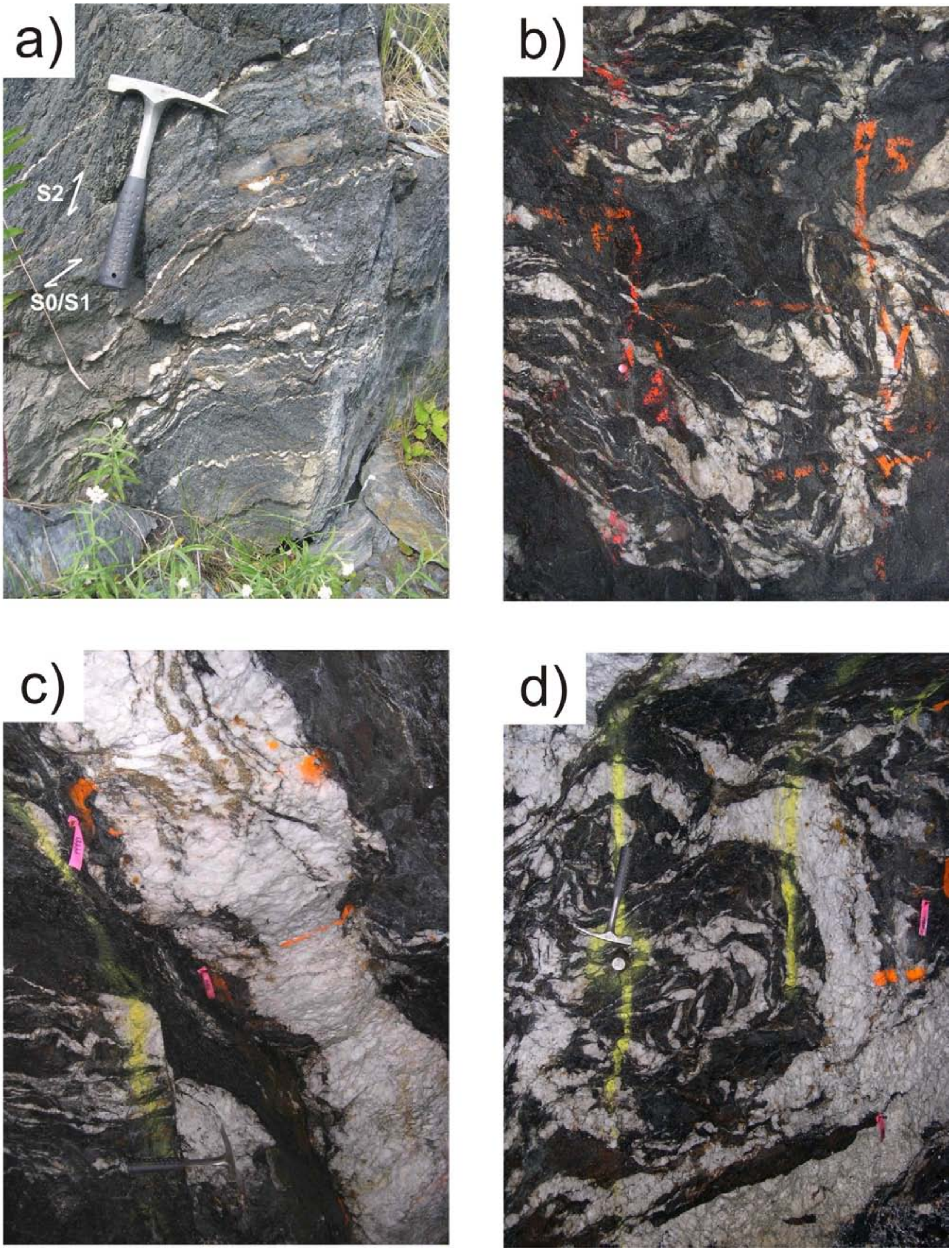
a)
S2
S0/S1
b)
c)
d)

Bloodgood (1987, 1992), and the existing K-Ar age is similar to the ages of earliest mineralization in the Wells-Barkerville area.

Ongoing Dating, Petrographic and Isotopic Studies at Frasergold

A K-Ar age of 151 ±5 Ma was reported by Panteleyev et al. (1996) for sericite from a mineralized quartz vein at the Frasergold occurrence. This is similar to $^{40}Ar/^{39}Ar$ ages obtained for mica grains from metamorphic rocks and early deformed quartz veins in the Wells-Barkerville area (discussed above), which would be consistent with the mineralized veins at Frasergold being older than most of the Au-bearing veins in the Wells-Barkerville area. This age remains to be corroborated by $^{40}Ar/^{39}Ar$ dating. During the fieldwork, a representative suite of samples for $^{40}Ar/^{39}Ar$ dating (n = 5) was collection from both underground and surface exposures and from drillcore, which included muscovite from veins, in vein selvages and from surrounding wallrock. Mineralized samples for the sulphide Pb isotope and detailed petrographic studies were also collected and will be analyzed as the project progresses.

Discussion: Initial Conclusions and Outstanding Questions

Our new $^{40}Ar/^{39}Ar$ ages from the Wells-Barkerville area indicate that early, deformed quartz veins were emplaced some time between 146.6 and 155.2 Ma, whereas both Au-bearing pyritic replacement deposits and extensional veins formed in the range of 138.5–147.6 Ma in latest Jurassic to earliest Cretaceous time. If these vein systems formed during, and in the waning stages of D_2 deformation as is interpreted, then these ages not only date the formation of the Au deposits and occurrences in the region but also constrain the timing of the D_2 event in the Barkerville terrane.

We recognize a separate deformation event in the Spanish Mountain area that occurred between the regionally defined D_1 (phase 1) and D_2 (phase 2) foliation forming events. Although an additional phase of folding between D_1 and D_2 has not been recognized in the Wells-Barkerville area, the intensity of the D_2 event in that area is sufficiently high that evidence for it may be obscured by overprinting deformation.

Although isotopic age data has not yet been obtained for Au-bearing veins in the Spanish Mountain area, the Au-bearing veins there exhibit similar geometries and timing relationships as vein systems in the Barkerville terrane. Based on similarities in vein style, orientations and suggested kinematics, and timing with respect to the dominant foliations, it is speculated that the Au-bearing extensional veins in the Wells-Barkerville area and the Spanish Mountain area occurred at the same time, probably in waning stages of D_2, and in response to shortening to the northeast, during initial formation of the north-trending dextral faults. Gold-bearing veins in the Frasergold area are clearly older than those at Spanish Mountain, but it is permissive that they formed at the same time as the early, deformed and locally Au-bearing quartz veins in the Wells-Barkerville area, and the early pyrite-quartz mineralization at Spanish Mountain. Although clearly related to discordant late faults in many parts of the Barkerville terrane, the commonly stratabound nature to these quartz veins also suggests a form of combined structural-stratigraphic control, where waning activity on D_2 thrusts could have contributed to the distribution of mineralized corridors within which discordant faults may have localized vein mineralization early in their history during a change in tectonic conditions.

Throughout most of the CGD, Au mineralization occurs dominantly in or associated with quartz veins, but the Wells-Barkerville area and Spanish Mountain deposit demonstrate their potential association with earlier, more sulphide-rich types of mineralization. If these early styles of mineralization are genetically related to the younger quartz-vein sets, they suggest that these deposits define zones of long-lived hydrothermal fluid flow that exploited common, but evolving fluid channelways. If so, the different styles of mineralization may reflect temporal changes in fluid composition, strain state, paleodepth and temperature spanning regional D_2 deformation. The spatial association also suggests the potential for early sulphide-rich styles of mineralization in areas where only quartz-vein deposits have been explored for thus far. It might be expected that

◄

Figure 14: Style of deformed vein systems in the Frasergold deposit: **a)** stratabound nature of deformed quartz veins in outcrop near Grouse Creek; the S_2 foliation is parallel to the rock hammer, and axial planar to folds of the veins; view northwest; **b)** folded, concordant extensional veins; view southeast in underground workings, field of view 2 m; **c)** a banded, southwest-dipping discordant vein, at the lower right, is joined in its hangingwall by folded, narrower semiconcordant quartz extensional veins; although folded by F_2 folds, the veins in the hangingwall of the larger vein display geometries compatible with development as sigmoidal extensional-vein arrays in the hangingwall of a larger shear vein; view northwest in underground workings; **d)** larger, steeply dipping 0.5 m wide white quartz veins with Au-bearing orange-brown iron-carbonate>pyrite bands; view southeast in underground workings; larger, 15–50 cm thick quartz-carbonate veins (Figure 14c) that are developed at moderate to high angles to S_0/S_1 are also associated with the concordant veins; these generally have higher iron-carbonate content than the smaller concordant veins, but contain the same blocky recrystallized white quartz fill; although thicker than the other veins, these veins are also discontinuous and may terminate laterally or vertically. These thicker veins are openly folded by folds with axial-planar S_2 foliation; highest grades (>3 g/t Au) commonly occur associated with the larger veins where they contain most abundant clots of iron-carbonate+pyrite, which may be aligned in discontinuous lenses of bands parallel to vein walls (Figure 14c); Au occurs both as relatively coarse, free grains associated with masses of iron-carbonate, pyrite and/or pyrrhotite within the veins and also as fine grains within quartz near vein margins.

these earlier pyritic forms of mineralization could vary in style depending on the hostrock, as is demonstrated by the variation from pervasive replacement of limestone seen at the Island Mountain and Mosquito deposits, to the coalescing series of pyritic veinlets with disseminated pyrite that comprises the siltstone-hosted Bonanza Ledge zone. If so, if more calcareous units are present in the Spanish Mountain stratigraphy, it is possible that these might also be preferentially replaced by pyrite associated with the early mineralizing event there.

Regional Indicators for Au Mineralization in the CGD

Carbonate alteration is widespread in all three Au-bearing areas that have been examined in the CGD. At Frasergold and Spanish Mountain, mineralized zones are characterized by the presence of distinctive 'knotted' schist textures caused by the presence of abundant iron-carbonate porphyroblasts. These porphyroblasts formed relatively early in the structural evolution of each area (syn-D_1 or early D_2). At Spanish Mountain, the carbonate porphyroblasts are widespread and extend well beyond mineralization, but they may reflect a broad peripheral effect to the alteration associated with the early pyrite-quartz mineralization. The porphyroblasts at Frasergold, however, could potentially represent an alteration effect related to the emplacement of the Au-bearing veins, since both the veins and the porphyroblasts formed early. It is interesting to note that very similar iron-carbonate porphyroblasts are closely associated with deformed Au-bearing quartz veins at both the Kusk Au occurrence 4 km to the south of Frasergold and the Forks occurrence 20 km to the northwest. 'Knotted' schist fabrics have not been reported thus far from any other localities within the Triassic black phyllite; thus this could represent a useful field criterion for identifying potentially Au-bearing zones in the region.

Rusty brown iron-carbonate alteration, commonly associated with disseminated pyrite, is also commonly associated with Au-bearing veins in the Wells-Barkerville area, where it occurs pervasively, often affecting feldspar in sandstone and siltstone beds and laminations over broad portions of the sequence surrounding the areas of veining in the Cariboo Gold Quartz and Island Mountain mines. Much of the fine-grained carbonaceous grey phyllite in the Wells area have no visible alteration if coarser beds are not present, except for local areas of carbonate and/or pyrite porphyroblast development.

In most of the lode-bearing portions of the Barkerville terrane, mineralization in late quartz veins and replacement mineralization are spatially associated with sets of early, deformed and boudinaged quartz-carbonate-muscovite veins. These are also abundant between Yanks Peak and Lightning Creek, where thick, blocky early quartz vein rubble is commonly exposed on ridgetops and in alpine areas, linking the Au-bearing domains at Yanks Peak and Lightning Creek. These associations suggest that quartz vein generations of all types, even if not significantly Au bearing, may be indicators of nearby, or along-strike areas of Au mineralization associated with later generations of quartz-vein mineralization.

Possible Role of Intrusions in Au Mineralization

Although all of the mineralization in the CGD is considered to be orogenic in style, intrusive rocks are present in the vicinity of Au mineralization in both the Spanish Mountain area and the Wells-Barkerville area. At Spanish Mountain, mafic (?) to felsic sill complexes dated at 185–187 Ma are spatially associated with the main mineralized area. The intrusions predate all deformation phases in the area and have been overprinted by the late carbonate-fuchsite alteration that appears to be associated with the mineralization. It is interesting, however, to note that the intrusions also coincide spatially with iron-carbonate porphyroblast development, raising the possibility that porphyroblast development, and possibly an early introduction of Au into the sedimentary sequence in this area, may have been associated with the emplacement of Early Jurassic intrusions. However, there is no evidence at this point for intrusions of this age in any of the other areas of iron-carbonate porphyroblast development and Au mineralization elsewhere in the Triassic black phyllite package (e.g., Frasergold).

Although both predeformation (Proserpine intrusions) and postdeformation (rhyolite and lamprophyre dikes) intrusions have been recognized in the Wells-Barkerville area, it seems unlikely that either of these intrusive events is related to the Au mineralization, although isotopic dating of the younger set of intrusions is now underway to test this.

Some of the problems that the authors are tackling in the CGD also bear directly on the origin of orogenic Au deposits globally. Work that is currently underway in two of the other main Phanerozoic orogenic Au districts in the world (Klondike Au belt, Yukon and Otago schist belt, New Zealand) by Mortensen and collaborators from the University of Otago (MacKenzie et al., 2007; Mortensen et al., unpublished data) has clearly demonstrated that at least two distinct end-members of orogenic Au deposits can be recognized on the basis of the source of metals and fluids involved. In the Otago schist belt in New Zealand, it has been shown convincingly that metals and fluids that formed orogenic Au veins were derived by metamorphic dehydration reactions across the greenschist-amphibolite facies transition at considerable depth beneath the mineralized region (e.g., Pitcairn et al., 2007). This is the most common genetic model for orogenic Au deposits espoused in the recent literature (e.g., Goldfarb et al., 2005). In the Klondike Au district in western Yukon, however, MacKenzie et al. (2008) and Mortensen (unpublished data) have shown that the metals contained within orogenic veins in that area are locally derived from a distinctive package of submarine felsic metavolcanic rocks that contain small, precious-metal–enriched VMS occurrences, and host or immediately underlie the vein systems. Vein-hosted Au mineralization in the Wells-Barkerville area closely resembles that in the Klondike Au district, and the intimate association between clusters of Au-bearing quartz veins and Au-rich hostrocks in different parts of the CGD (Au-bearing pyritic mantos in the Wells-Barkerville area and disseminated Au in altered metaclastic rocks at Spanish Mountain) argues that the CGD likely has more in common with the Klondike Au district than with the Otago schist belt.

Dunne et al. (2001) carried out a reconnaissance level fluid inclusion study of Au-bearing quartz veins in the Wells-Barkerville area. An extensive suite of samples of vein quartz for fluid inclusion analysis was collected from throughout the CGD during the course of the 2008 fieldwork program. These samples will form the basis for a fluid chemistry study that is currently planned of Au-bearing veins in the Barkerville terrane and lower portions of the Quesnel terrane by Mortensen and colleagues from the University of Leeds. In addition, compositional data for placer- and lode-Au samples from throughout the CGD that were reported by McTaggart and Knight (1993) are currently being reinterpreted and additional compositional work on the McTaggart and Knight sample suite is underway. This will include work on additional lode-Au samples that were collected during 2008.

There are some outstanding questions regarding lode-Au deposits and potential in the CGD:

- What are the absolute ages of, and relationships between, Au-bearing veins and earlier pyrite mineralization in the CGD?
- If related, are they part of a coeval or temporally transgressive mineralizing event across the district now exposed at different structural levels?
- What are the ages of Au-bearing veins at the Frasergold deposit, and are they related to older forms of mineralization that are observed elsewhere in the district?
- What are the specific structural controls on mineralization in each of these areas, and is there evidence for interaction between late D_2 thrust activity and younger faults that localized mineralization?
- What is the nature and source of the metals and mineralizing fluids in each camp?

The authors' ongoing research in the CGD is directed at these and other key questions. It is believed that resolving these questions will provide valuable new insights into the nature and origin of Au in the CGD, and will result in new exploration criteria that can be applied to ongoing exploration efforts not only within the CGD, but also elsewhere in BC.

Acknowledgments

This project is funded by Geoscience BC with matching support from Hawthorne Gold Corporation, Skygold Ventures Ltd. and International Wayside Gold Mines Ltd. The authors are extremely grateful for the hospitality, logistical support and access provided by all three of these companies during the fieldwork component of this study that was conducted in August. F. Callaghan of International Wayside Gold Mines Ltd. is particularly thanked for funding the use of a helicopter, which allowed the authors to access areas within the Barkerville terrane that would otherwise have been inaccessible during the duration of the fieldwork program. Rhys and Ross also would like to acknowledge the companies' permission to draw from the results of previous consulting work they conducted in the region. The manuscript has benefited from editorial reviews by J. Logan and B. Singh.

References

Alldrick, D.J. (1983): The Mosquito Creek mine, Cariboo gold belt (93H/4); *in* Geological Fieldwork 1982, BC Ministry of Energy, Mines and Petroleum Resources, Paper 1983-1, p. 99–112.

Andrew, A., Godwin, C.I. and Sinclair, A.J. (1983): Age and genesis of Cariboo gold mineralization determined by isotope methods (93H); *in* Geological Fieldwork 1982, BC Ministry of Energy, Mines and Petroleum Resources, Paper 1983-1, p. 305–313.

Ash, C.H. (2001): Relationship between ophiolites and gold-quartz veins in the North American Cordillera; BC Ministry of Energy, Mines and Petroleum Resources, Bulletin 108, 140 p.

Belik, G.D. (1988): Percussion drilling report on the Kusk 5 and Kusk A mineral claims, Cariboo Mining Division, British Columbia; BC Ministry of Energy, Mines and Petroleum Resources, Assessment Report 18 025, 12 p.

Benedict, P.C. (1945): Structure at the Island Mountain mine, Wells, British Columbia; Transactions, Canadian Institute of Mining and Metallurgy, v. 48, p. 755–770.

Bloodgood, M.A. (1987): Deformational history, stratigraphic correlations and geochemistry of eastern Quesnel Terrane rocks in the Crooked Lake area, central British Columbia, Canada; M.Sc. thesis, University of British Columbia, 165 p.

Bloodgood, M.A. (1992): Geology of the Eureka Peak and Spanish Lake map areas, British Columbia; BC Ministry of Energy, Mines and Petroleum Resources, Paper 1990-3, 36 p.

Delancey, P. (1988): 1987 Cunningham Creek property report; British Columbia; BC Ministry of Energy, Mines and Petroleum Resources, Assessment Report 17 114, 26 p.

Dunne, K.P.E., Ray, G.E. and Webster, I.C.L. (2001): Preliminary fluid inclusion study of quartz vein and massive banded stringer pyrite mineralization in the Barkerville gold camp, east-central British Columbia; *in* Geological Fieldwork

2000, BC Ministry of Energy, Mines and Petroleum Resources, Paper 2001-1, p. 169–190.

Ferri, F. and Friedman, R.M. (2002): New U-Pb and geochemical data from the Barkerville subterrane; *in* Slave-northern Cordillera Lithospheric Evolution (SNORCLE) Transect and Cordilleran Tectonics Workshop meeting, LITHOPROBE Report 82, p. 75–76.

Ferri, F. and Schiarizza, P. (2006): Reinterpretation of the Snowshoe Group stratigraphy across a southwest-verging nappe structure and its implications for regional correlations within the Kootenay Terrane; *in* Paleozoic Evolution and Metallogeny of Pericratonic Terranes at the Ancient Pacific Margin of North America, M. Colpron and J.L. Nelson (ed.), Canadian and Alaskan Cordillera: Geological Association of Canada, Special Paper 45, p. 415–432.

Ferri, F., Höy, T. and Friedman, R.M. (1999): Description, U-Pb age and tectonic setting of the Quesnel Lake gneiss, east-central British Columbia; *in* Geological Fieldwork 1998, BC Ministry of Energy, Mines and Petroleum Resources, Paper 1999-1, p. 69–80.

Godwin, C.I. and Sinclair, A.J. (1982): Average lead isotope growth curves for shale-hosted zinc-lead deposits, Canadian Cordillera; Economic Geology, v. 77, p. 675–690.

Goldfarb, R.J., Baker, T., Dube, B., Groves, D.I., Hart, C.J.R. and Gosselin, P. (2005): Distribution, character, and genesis of gold deposits in metamorphic terranes; *in* Economic Geology 100th Anniversary Volume, J.W. Hedenquist, J.F.H. Thompson, R.J. Goldfarb and J.P. Richards (ed.), Society of Economic Geologists, Inc., p. 407–450.

Goodall, G. and Campbell, K. (2007): Summary report and exploration potential on the Frasergold Project; NI43-101 Report for Hawthorne Gold Corporation, 51 p.

Hall, R. D. (1999): Cariboo gold project at Wells, British Columbia; International Wayside Gold Mines Limited, URL <http://www.wayside-gold.com/i/pdf/RHall_report.pdf> [November 2008], 52 p.

Holland, S.S. (1954): Geology of the Yanks Peak–Roundtop Mountain area, Cariboo District, British Columbia; BC Ministry of Energy, Mines and Petroleum Resources, Bulletin 34, 102 p.

Howard, D.A. (1989): Geological, diamond drilling and trenching results from the 1988 exploration program on the Forks 1-4, AR 1-2, TEP 1-3 claims, Cariboo Mining Division, MacKay River District, British Columbia; BC Ministry of Energy, Mines and Petroleum Resources, Assessment Report 18 471, 45 p.

Johnston, W.A. and Uglow, W.L. (1926): Placer and vein deposits of Barkerville, Cariboo District, British Columbia; Geological Survey of Canada, Memoir 149, 246 p.

Levson, V.M. and Giles, T.R. (1993): Geology of Tertiary and Quaternary gold-bearing placers in the Cariboo region, British Columbia (93A, B, G, H); BC Ministry of Energy, Mines and Petroleum Resources, Bulletin 89, 202 p.

Logan, J., (2008): Geology and mineral occurrences of the Quesnel Terrane, Cottonwood map sheet, central British Columbia (NTS 093G/01); *in* Geological Fieldwork 2007, BC Ministry of Energy, Mines and Petroleum Resources, Paper 2008-1, p. 69–86.

MacKenzie, D., Craw, D. and Mortensen, J.K. (2007): Structural controls on orogenic gold mineralisation in the Klondike goldfield, Canada; Mineralium Deposita, doi:10.1007/s00126-007-0173-z.

MacKenzie, D., Craw, D., Mortensen J.K. and Liverton, T. (2008): Disseminated gold mineralization associated with orogenic veins in the Klondike schist, Yukon; *in* Yukon Exploration and Geology 2007, D.S. Emond, L.R. Blackburn, R.P. Hill and L.H. Weston (ed.), Yukon Geological Survey, p. 215–224.

McTaggart, K.C. and Knight, J. (1993): Geochemistry of lode and placer gold of the Cariboo District, B.C.; BC Ministry of Energy, Mines and Petroleum Resources, Open File 1993-30, 24 p.

Mortensen, J.K., Ghosh, D. and Ferri, F., 1995, U-Pb age constraints of intrusive rocks associated with Copper-Gold porphyry deposits in the Canadian Cordillera; *in* Porphyry Deposits of the Northwestern Cordillera of North America, T.G. Schroeter (ed.), CIM Special Volume 46, p. 142–158.

Mortensen, J.K., Montgomery, J.R. and Fillipone, J. (1987): U-Pb zircon, monazite and sphene ages for granitic orthogneiss of the Barkerville Terrane, east-central British Columbia; Canadian Journal of Earth Sciences, v. 24, p. 1261–1266.

Panteleyev, A., Bailey, D.G., Bloodgood, M.A. and Hancock, K.D. (1996): Geology and mineral deposits of the Quesnel River–Horsefly map area, central Quesnel Trough, British Columbia (NTS map sheets 93A/5, 6, 7, 11, 12, 13; 93B/9, 16; 93G/1; 93H/4); BC Ministry of Energy, Mines and Petroleum Resources, Bulletin 97, 156 p.

Pickett, J.W. (2001): Diamond drilling and geochemical soil sampling report on a portion of the IGM Group of mineral claims; BC Ministry of Energy, Mines and Petroleum Resources, Assessment Report 26 492, 57 p.

Pitcairn, I.K., Teagle, D.A.H., Craw, D., Olivo, G.R., Kerrich, R.T. and Brewer, T.S. (2007): Sources of metals and fluids in orogenic gold deposits: insights from the Otago and Alpine schists, New Zealand; Economic Geology, v. 101, p. 1525–1546.

Ray, G.E., Webster, I.C.L., Ross, K. and Hall, R. (2001): Geochemistry of auriferous pyrite mineralization at the Bonanza Ledge, Mosquito Creek mine and other properties in the Wells-Barkerville area, British Columbia; *in* Geological Fieldwork 2000, BC Ministry of Energy and Mines, Paper 2001-1, p. 135–167.

Rees, C.J. (1987): The Intermontane-Omineca Belt boundary in the Quesnel Lake area, east-central British Columbia: tectonic implications based on geology, structure and paleomagnetism; Ph.D. thesis, Carleton University, 421 p.

Rhys, D.A. and Ross, K.V. (2001): Evaluation of the geology and exploration potential of the Bonanza Ledge zone, and adjacent areas between Wells and Barkerville, east-central British Columbia; internal company report prepared for International Wayside Gold Mines Ltd., URL <http://www.wayside-gold.com/i/pdf/Rhys-Ross-2001.pdf> [November 2008], 110 p.

Richards, F. (1948): Cariboo Gold Quartz mine; *in* Structural Geology of Canadian Ore Deposits, Canadian Institute of Mining and Metallurgy, p. 162–168.

Robert, F. and Taylor, B.E. (1989): Structure and mineralization at the Mosquito Creek gold mine, Cariboo District, B.C.; *in* Structural Environment and Gold in the Canadian Cordillera, Geological Association of Canada, Cordilleran Section, Short Course no. 14, p. 25–41.

Ross, K.V. (2006): Petrographic study of the Spanish Mountain project, Cariboo Mining District; internal company report prepared for Skygold Ventures Ltd., 64 p.

Schiarizza, P. (2004): Bedrock geology and lode gold occurrences, Cariboo Lake to Wells, British Columbia, parts of NTS 93A/13, 14; 93H/3, 4; BC Ministry of Energy, Mines and Petroleum Resources, Open File 2004-12, 1:100 000 scale.

Schiarizza, P. and Ferri, F. (2003): Barkerville Terrane, Cariboo Lake to Wells: a new look at stratigraphy, structure and regional correlations of the Snowshoe Group; *in* Geological Fieldwork 2002, BC Ministry of Energy, Mines and Petroleum Resources, Paper 2003-1, p. 79–96.

Skerl, A.C. (1948): Geology of the Cariboo Gold Quartz mine; Economic Geology, v. 43, p. 571–597.

Singh, B. (2008): Technical report on the Spanish Mountain property for Skygold Ventures Ltd.; NI43-101 report filed on SEDAR, 92 p.

Struik, L.C. (1987): The ancient western North American margin: an Alpine rift model for the east-central Canadian Cordillera; Geological Survey of Canada, Paper 87-15, 19 p.

Struik, L.C. (1988): Structural geology of the Cariboo Gold Mining District, east-central British Columbia; Geological Survey of Canada, Memoir 421, 100 p.

Sutherland Brown, A. (1957): Geology of the Antler Creek area, Cariboo District, British Columbia; BC Ministry of Energy, Mines and Petroleum Resources, Bulletin 38, 105 p.

Termuende, T. (1990): Geological report on the Craze Creek (Cunningham) property for Loki Gold Corporation; BC Ministry of Energy, Mines and Petroleum Resources, Assessment Report 19 793, 21 p. plus maps.

Yin, J. and Daignault, P. (2007): Report on the 2006 exploration program on the Golden Cariboo project, Wells, B.C.; BC Ministry of Energy, Mines and Petroleum Resources, Assessment Report 28 990, 44 p.